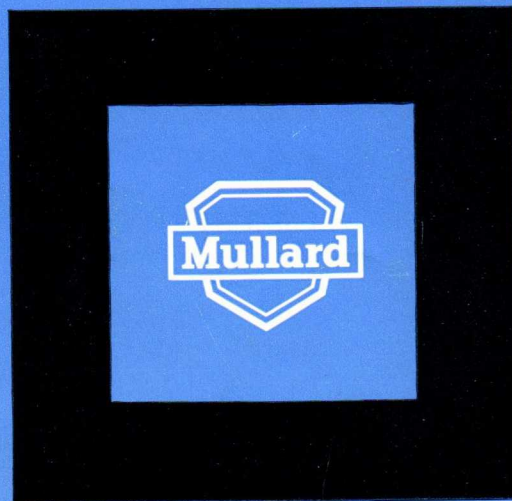
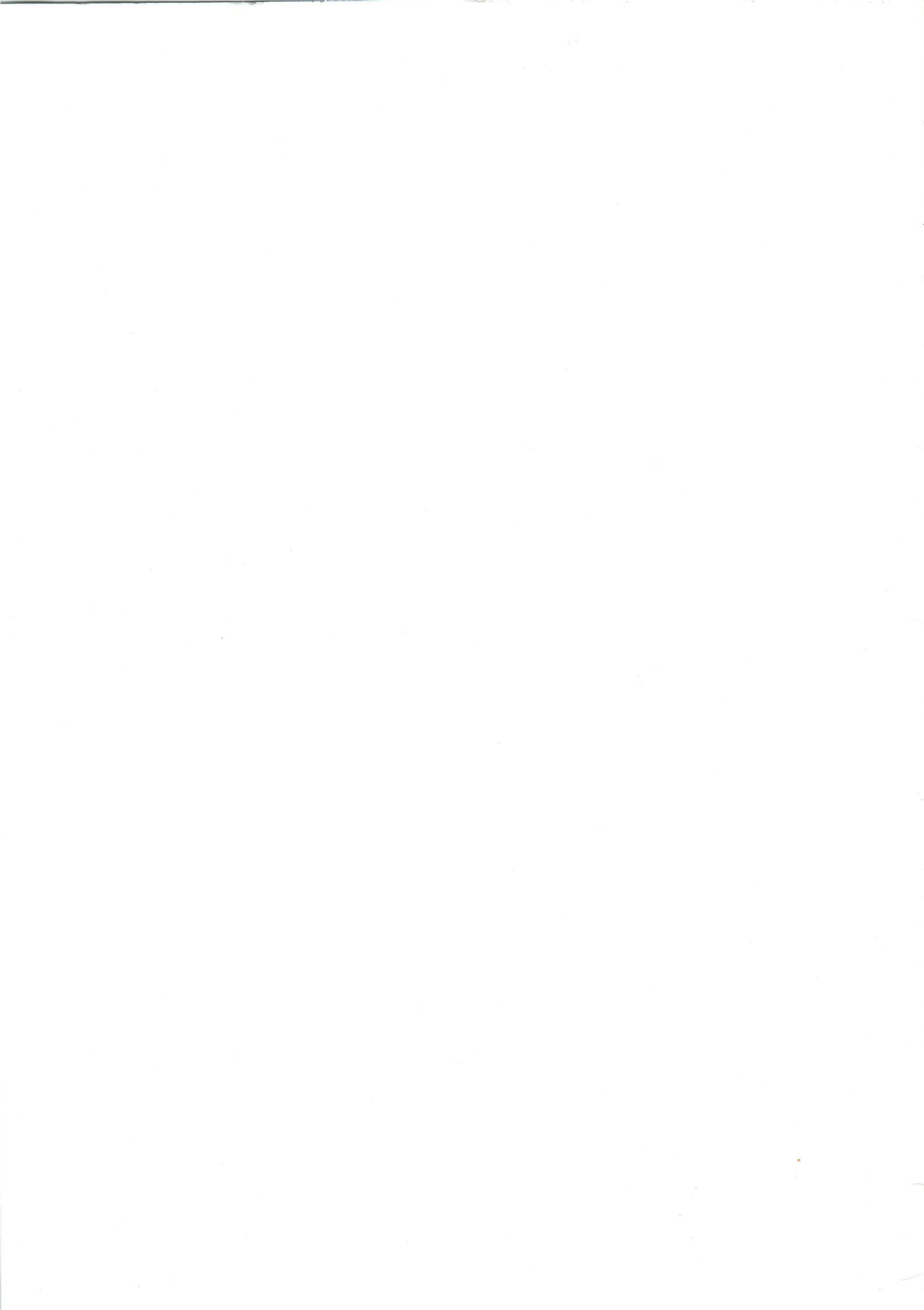


**Mullard** Technical Communications

SplitHubox

VOLUME 7 NUMBER 66 August 1963





# Mullard Technical Communications

VOLUME 7 NUMBER 66 August 1963

<b>Contents</b>	Elimination of Switch-off Spots in TV Receivers <i>C. E. Longhurst</i>	170
	Junction Temperature of Diodes in Harmonic Generators <i>G. D. Bergman</i>	172
	Design of High-impedance Common-collector Input Stages <i>A. J. Tumber</i>	175
	Dual Trace Oscilloscope Tubes <i>E. J. Grodzinsky</i>	179
	Trigger Tube Coupling Circuits for Counting Tubes <i>G. F. Jeynes and S. Zilkha</i>	184
	Electrometer Valves <i>S. S. Dagpunar</i>	194

---

*Mullard Technical Communications* contains information on the performance or application of Mullard products such as electronic valves and tubes, semiconductor devices, and electrical and magnetic components. It is issued free-of-charge to equipment designers, research organisations, reference libraries, and educational establishments. Bona fide applications to be added to the circulation list should be made under an official letter head to the Technical Information Department. Overseas enquiries should be addressed to the local Mullard agent, or to Mullard Overseas Ltd. at Mullard House.

Abstracts, or references to an article, should mention both the source, *Mullard Technical Communications*, and the authors. Requests for republication or translation should be made to the Editor in writing.

The issue of the information contained in this publication does not imply any authority or licence for the utilisation of any patented feature.

'Mullard' is the trade mark of Mullard Limited and is registered in most of the principal countries of the world.

Editor: F. A. Sowan

Assistant Editors: E. G. Evans R. Barrie

*Published by*

Technical Information Department  
Mullard Limited, Mullard House, Torrington Place, London, W.C.1  
LANgham 6633

© Mullard Limited, 1963

*Made and Printed in England by*  
WIGHTMAN AND COMPANY LIMITED, 1/3 BRIXTON ROAD, LONDON, S.W.9

# Elimination of Switch-off Spots in TV Receivers

C. E. LONGHURST

Mullard Research Laboratories

*It is desirable that a television receiver should not exhibit a spot at switch-off. This is best achieved by ensuring a rapid discharge of the e.h.t. capacitance and is most conveniently accomplished by using the picture tube as a discharge device. It is essential to ensure that the timebases provide some scan during the discharge time. Three methods of achieving spot suppression at switch-off, using a minimum of components, are given. These precautions, however, do not afford protection under fault conditions.*

## INTRODUCTION

When a television receiver is switched off, there sometimes appears at the centre of the screen (depending upon design features of that particular circuit) a bright spot of diminishing luminance. This spot generally causes concern to the average viewer. It is also a potential source of danger to the screen because the spot occasionally is of sufficient intensity and duration to cause localised phosphor discoloration.

The spot is the result of a residual charge being retained by the e.h.t. filtering capacitance, after the receiver is switched off. This charge maintains an accelerating potential on the final tube anode, and since the tube cathode remains hot for some time after switch-off, the electrons which are emitted are accelerated. Since there are no deflecting fields, the electrons strike the screen centrally causing a brilliant local luminescence. The effective area of such a spot will depend on the h.t. time-constants of both the e.h.t. and deflection circuits. In order to ensure that a switch-off spot will not occur irrespective of the picture-content or viewer control settings just prior to switch-off, one of two methods can be utilised:

- (i) discharging the residual e.h.t. charge immediately on switching off the receiver,
- (ii) biasing the tube off at switch-off and maintaining the bias until the tube cathode has cooled sufficiently to cease emitting electrons.

## CIRCUIT REQUIREMENTS

The rate of decay of the pertinent potentials on the tube at switch-off will either encourage the discharge of the e.h.t. reservoir capacitor by the flow of beam current, or bias the tube off. The requirements for either of these two conditions to occur are given below.

To discharge the e.h.t. capacitor, the cathode potential should decay more rapidly than the control grid, thus encouraging the flow of beam current and hence discharg-

ing the e.h.t. capacitor. At the same time the first anode potential must be maintained.

When the technique of using the picture tube as the discharge device is adopted, it is essential that the timebases should provide some scan until the discharge is completed. In this way the beam current is distributed over a reasonable screen area and discoloration is prevented. Thus, long time-constants for these circuits are desirable. In this respect, a particularly important time-constant is that of the h.t. supply to the vertical oscillator. In most receivers this supply is obtained from the line timebase boost potential and failure of the line circuit will, unless the smoothing time-constant for the vertical oscillator is adequate, cause the cessation of the vertical oscillator. Furthermore, to minimise the danger of spot burn under fault conditions, separate h.t. smoothing for the line and field timebases is advantageous.

To bias the tube off, the control grid must be maintained negative with respect to the cathode or the cathode positive with respect to the grid after switch-off, until the cathode cools and ceases to emit electrons. This condition is very difficult to fulfil since the cathode remains hot for a considerable period and receivers employing this technique tend to produce a spot shortly after switch-off.

A further disadvantage is that the charged e.h.t. capacitance can present a hazard to service engineers since cathode ray tubes are capable of retaining their charge for considerable periods. The use of a 'leak' resistor to discharge the e.h.t. capacitance has not, in the past, proved practicable. Voltage dependent resistors, which have previously been used as e.h.t. stabilising devices, are not ideally suited to this application because of their unfavourable non-linear voltage characteristics.

It is therefore apparent that the most satisfactory technique is that of employing the picture tube as the discharge device. To minimise the relevant time-constants, it is necessary for the tube to be driven hard into conduction, as soon as the receiver is switched off.

In all methods for which the tube is used as the discharge device, it is necessary that the potential on the first accelerating anode should be maintained as long as possible after switch-off. This is because these methods rely on an increased beam current to discharge the e.h.t. capacitance and, in order to accomplish the discharge, electrons must be drawn from the still hot cathode. Thus, the time-constant associated with the first anode should be longer than the time-constants associated with the grid and cathode of the picture tube, and also the scanning circuits.

**DISCHARGING THE E.H.T. CAPACITANCE**

If the control grid of the picture tube is connected to a large positive potential at switch-off, the tube will be driven hard into conduction. Provided that the series grid resistor limits the grid current to a safe value, the amplitude and waveform are unimportant. Therefore, the supply mains can be used.

A simple circuit arrangement is to return the lower end of the brightness control chain to the neutral line on the permanently live side of the mains switch of the receiver, when a large 50c/s component will be fed to the control grid of the c.r.t. at switch-off. Beam current flows at the mains frequency and the e.h.t. capacitor is discharged. This arrangement is shown in Fig. 1.

There is a disadvantage in this arrangement in that the receiver is floating at some high undetermined potential when switched off. This applies particularly if there is no indication on the mains supply to differentiate between the neutral and live lines. A further disadvantage is that the system operates only when the normal receiver on-off switch is used.

In some European countries safety regulations prohibit this method of e.h.t. discharge, but this technique is very satisfactory, not only because of its efficiency but also because it requires no extra components.

**MODIFICATION OF THE CONTROL GRID POTENTIAL DECAY TIME**

Voltage dependent resistors (v.d.r.) possess the property of increasing resistance with decreasing applied potential. They thus tend to stabilise a potential against change and can effectively lengthen the time-constant of a circuit. If a v.d.r. is inserted in the brightness control chain as shown in Fig. 2, the control grid potential is maintained even though the h.t. potential diminishes at switch-off. The grid is therefore held at a more positive potential than the cathode, and the e.h.t. charge is discharged by the flow of beam current before the scanning fields collapse.

To provide a satisfactory range of brightness control for all picture tubes, the control grid must be able to swing to an adequate negative potential with respect to the cathode. A limitation of this method is that the d.c. potential across the v.d.r. sets a minimum value for the control grid potential.

**LINE-PULSED V.D.R. CIRCUIT**

A development of the previous circuit (Fig. 2) is to use the v.d.r. to rectify positive-going line flyback pulses to produce a negative bias. The circuit is shown in Fig. 3. The non-linear v.d.r. acts as a diode, developing a negative potential at its top end. This potential is applied to the lower end of the brightness control as shown in Fig. 3. Modulation of the grid potential by line pulses is prevented by the smoothing capacitor  $C_2$ . Since this capacitor has only to bypass the line pulses, a low value is adequate and thus a short grid time-constant is obtained.

At switch-off the negative potential decreases, thereby tending to increase the control grid potential in a positive

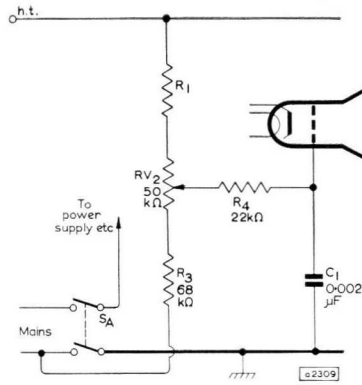


Fig. 1—Grid of the c.r.t. connected to a large positive potential at switch-off, thus driving the tube into conduction

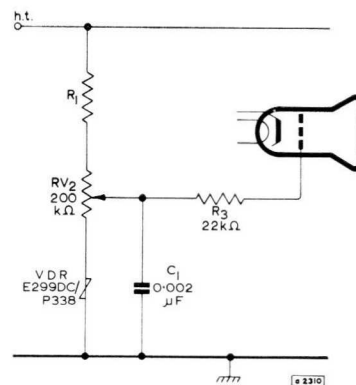


Fig. 2—Control grid potential maintained at switch-off by means of a v.d.r.

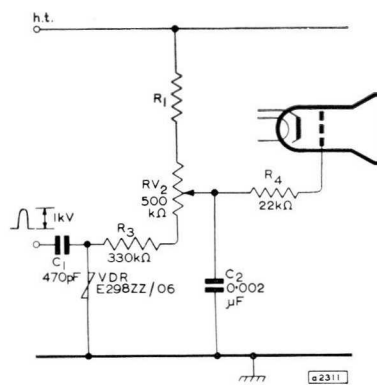


Fig. 3—Positive-going line flyback pulses rectified to produce a negative bias by means of a v.d.r.

direction. In addition, the impedance of the v.d.r. increases, which drives the control grid even further positive, resulting in rapid discharge of the e.h.t. capacitance, again by means of beam current.

The choice of v.d.r. is not critical, since it is only necessary to develop a negative potential for application to the lower end of the brightness control. A pulse of about 1kV is normally readily available from the line transformer, and the v.d.r. is selected to provide a bias of approximately  $-150V$  across itself.

# Junction Temperature of Diodes in Harmonic Generators

G. D. BERGMAN

Wembley Laboratories, Associated Semiconductor Manufacturers Ltd.

*The dissipation of silicon variable-capacitance diodes operating in harmonic generators cannot usually be simply calculated. To protect the diodes from overheating, it is necessary to measure the diode junction temperature under u.h.f. conditions. A practical system for making this measurement is described.*

## INTRODUCTION

Silicon variable-capacitance diodes like the SVC11 to SVC17 series are being used in increasing numbers in harmonic generators in the microwave frequency range. Optimum performance in this type of harmonic generator is attained to a large extent by empirical methods, and in a practical circuit it is often difficult to calculate the amount of power that is being dissipated in the diode. Measurement of conversion loss gives only an indication of this power, since the losses in any system are not solely due to the diode.

Since semiconductor diodes of this type are susceptible to damage by overheating, it is important to have a means of assessing the power dissipated, in order to ensure that this power does not exceed the rating assigned to it. A technique has been devised for measuring the junction temperature of a variable-capacitance diode in a harmonic generator circuit. From the junction temperature rise above ambient and a knowledge of the thermal resistance, it is possible to calculate the power dissipated in the diode. In this article the technique is described, and is illustrated by its application to measurements on a practical harmonic generator.

## MEASURING TECHNIQUE

The method of measuring junction temperature is based upon the temperature variation of the forward voltage of a diode at a constant forward current. At fairly low current levels, silicon diodes exhibit a voltage variation of roughly 2mV/degC at constant forward current. This characteristic is employed to measure the junction temperature of a diode in a harmonic generator circuit by means of the switching circuit shown schematically in Fig. 1. Most of the time, switch  $S_A$  is closed, thus holding the diode under test (which is connected in a harmonic generator circuit) to an appropriate reverse bias voltage  $V_B$ . Switch  $S_B$  is normally open, and switch  $S_C$  is connected to point Q which is at a preset reference voltage.

With the switches in these positions, microwave power is supplied to the diode under test, causing its junction

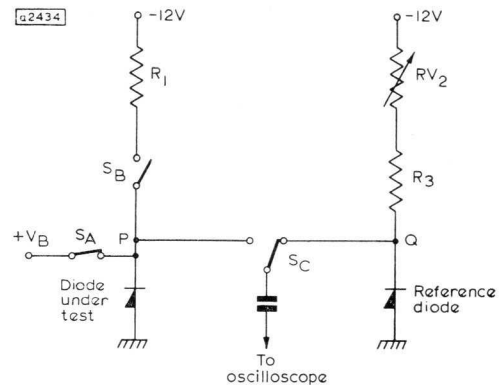


Fig. 1—Basic switching circuit

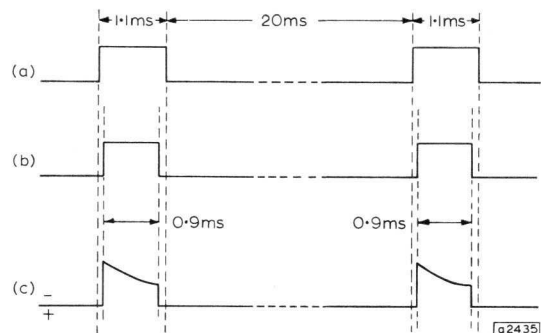


Fig. 2—Observed waveforms  
(a) output from  $W_1$ ,  $W_2$ , and  $W_5$   
(b) output from  $W_3$  and  $W_4$   
(c) oscilloscope waveform

temperature to rise above ambient. Repetitively, about once every 20ms, switch  $S_A$  is opened,  $S_B$  is closed, and  $S_C$  is connected to point P for about 1ms. For this same period it is arranged that the microwave power is turned off repetitively. During this period, reverse bias is removed from the diode under test, and the diode is biased in the forward direction with a current determined by  $R_1$ . This current is set to be about 10mA.

An a.c. output signal, consisting of a square waveform, is displayed on an oscilloscope. The magnitude of this signal is set by  $RV_2$  to zero when no power is dissipated in the diode under test and its junction is at ambient temperature. When power is dissipated in the diode, the magnitude of the square wave is a measure of the rise in its junction temperature above ambient, as it represents the difference between the forward voltage of the diode and a preset voltage. The appearance of the oscilloscope

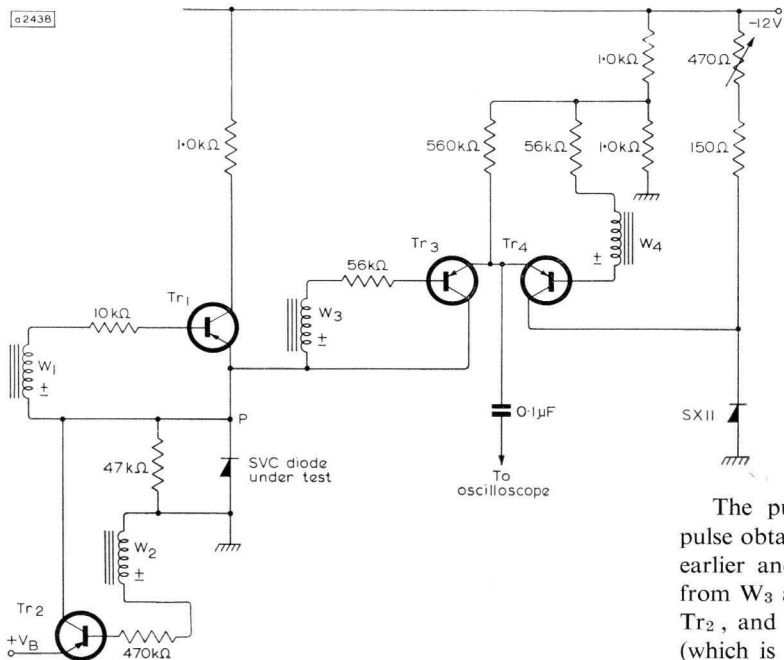


Fig. 3—Practical switching circuit  
Tr<sub>1</sub> to Tr<sub>4</sub>; GET103

waveform is as shown in Fig. 2c. There is a slight drop in the voltage as the diode cools down.

**PRACTICAL CIRCUIT**

The schematic circuit shown in Fig. 1 is realised in practice by the circuit shown in Fig. 3, the switching operations being performed by the transistors Tr<sub>1</sub> to Tr<sub>4</sub>. Transistor Tr<sub>2</sub> performs the operation of S<sub>A</sub>; Tr<sub>1</sub> performs the operation of S<sub>B</sub>; and Tr<sub>3</sub> and Tr<sub>4</sub> perform the operation of S<sub>C</sub>.

These last two transistors are reverse connected so that their saturation voltages are low. This is necessary because the temperature-measuring signal has a magnitude of only a few tens of mV, and any unequal variations

The pulse circuit is designed so that the switching pulse obtained from W<sub>1</sub>, W<sub>2</sub>, and W<sub>5</sub> starts about 0.1ms earlier and finishes 0.1ms later than the pulse obtained from W<sub>3</sub> and W<sub>4</sub>. This enables the switching of Tr<sub>1</sub> and Tr<sub>2</sub>, and also the switching-off of the microwave source (which is performed by the pulse from W<sub>5</sub>), to be completed before the measurement of forward voltage by means of Tr<sub>3</sub> takes place. This prevents any switching transients appearing in the output waveform to the oscilloscope.

The pulse generator shown in Fig. 3 is of conventional design. The basic repetition rate is established by means of a free-running multivibrator consisting of Tr<sub>1</sub> and Tr<sub>2</sub>. The repetition frequency can be varied by means of a variable resistor. The output pulses are generated by two bistable circuits, Tr<sub>3</sub> and Tr<sub>4</sub>, and Tr<sub>5</sub> and Tr<sub>6</sub>, which are triggered by the multivibrator. An output pulse of about 1.1ms duration is given by Tr<sub>3</sub> and Tr<sub>4</sub>.

The triggering to Tr<sub>5</sub> and Tr<sub>6</sub> is delayed for 0.1ms by means of R<sub>1</sub> and C<sub>1</sub>. Diode D<sub>3</sub> is used to discharge C<sub>1</sub>

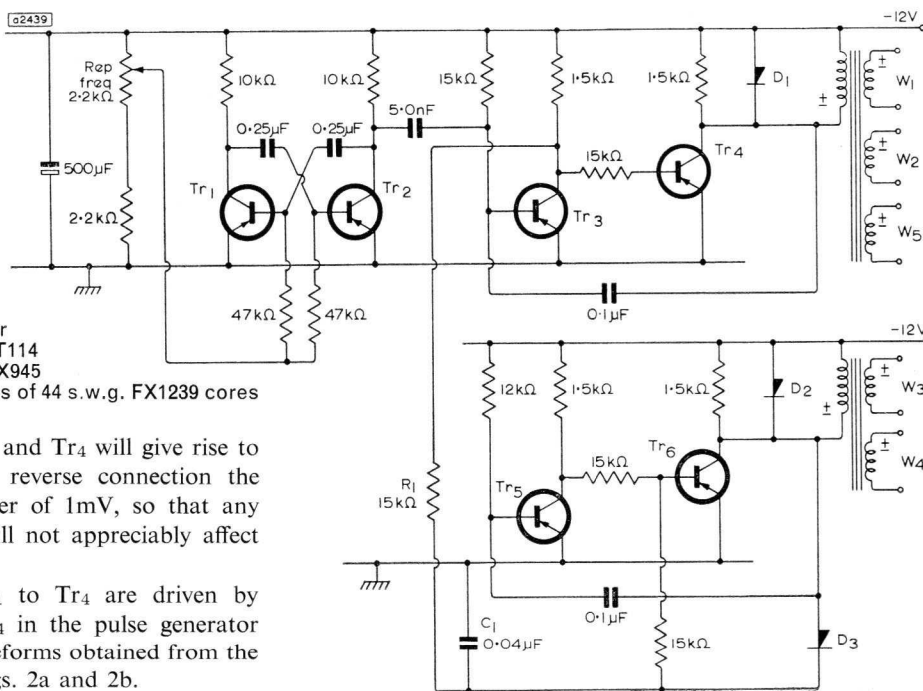


Fig. 4—Pulse generator  
Tr<sub>1</sub> to Tr<sub>6</sub>; GET114  
D<sub>1</sub> to D<sub>3</sub>; GEX945

All transformer windings: 1000 turns of 44 s.w.g. FX1239 cores

in the saturation voltages of Tr<sub>3</sub> and Tr<sub>4</sub> will give rise to errors of measurement. In the reverse connection the saturation voltage is of the order of 1mV, so that any changes in saturation voltage will not appreciably affect the signal being measured.

The bases of transistors Tr<sub>1</sub> to Tr<sub>4</sub> are driven by transformer windings W<sub>1</sub> to W<sub>4</sub> in the pulse generator circuit shown in Fig. 4. The waveforms obtained from the pulse generator are shown in Figs. 2a and 2b.

once triggering has taken place. The output pulse is about 0.9ms in duration. In this way the waveforms shown in Figs. 2a and 2b are produced.

**MEASUREMENTS**

A number of SVC11 series diodes have been calibrated in this measuring circuit, the diodes being heated to known junction temperatures by means of an oil bath. A curve showing the typical variation of output signal with rise in junction temperature is given in Fig. 5. This corresponds to a temperature coefficient of forward voltage of 1.66mV/degC.

It is found that, to an accuracy of  $\pm 2\%$ , this coefficient can be applied to all diodes. If greater accuracy of temperature measurement is required, individual calibration of diodes is necessary.

The output voltage gives a measure of the rise of junction temperature above ambient. Since this voltage is the difference between the voltage drop of the SVC diode heated by microwave power and a normal SX11 silicon junction diode at ambient temperature, the system is self-compensating for changes in ambient temperature, as the SX11 has roughly the same temperature coefficient of variation of forward voltage as the SVC diodes.

For a known rise in diode junction temperature above ambient it is possible to make an estimate of the power dissipated in the diode. For an SVC11 to SVC17 series diode mounted in a coaxial holder, the thermal resistance is  $43 \pm 5 \text{ degC/W}$ . The power dissipated in the diode is calculated by dividing the measured junction temperature rise by the thermal resistance. As there is a spread in thermal resistance, the thermal resistance of an individual diode is not known precisely unless it is specially measured. As a consequence, there is a possible error of  $\pm 10\%$  in this technique of power measurement.

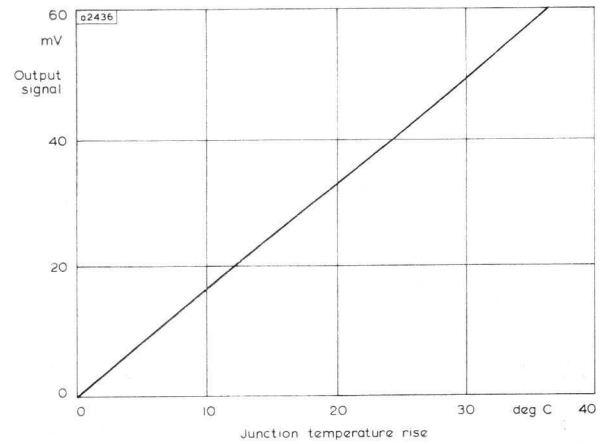


Fig. 5—Variation of output signal with junction temperature rise above ambient

**APPLICATION TO PRACTICAL CIRCUIT**

In Fig. 6 is shown the circuit arrangement that has been used for measuring the junction temperature of a diode in a 2.25Gc/s to 4.5Gc/s frequency doubler.

For the tests, a disc-seal triode oscillator was used which employed a TD03-10 u.h.f. triode. A transistor circuit was connected to the cathode of the triode, which reverse-biased it on receipt of a negative pulse from winding  $W_5$  (Fig. 4). This turned off the source of power and allowed temperature measurement of the variable capacitance diode to be made. The connections to the diode under test, as shown, are right for the SVC11 to SVC17, but must be reversed for the SVC21 and SVC22.

With this equipment it is possible to observe the junction temperature of the variable-capacitance diode while adjustments are made to the matching circuits and while the input power is varied. In this way the circuit has proved useful in making final adjustments to the harmonic generator, and ensuring that under no conditions is the temperature rating of the diode exceeded.

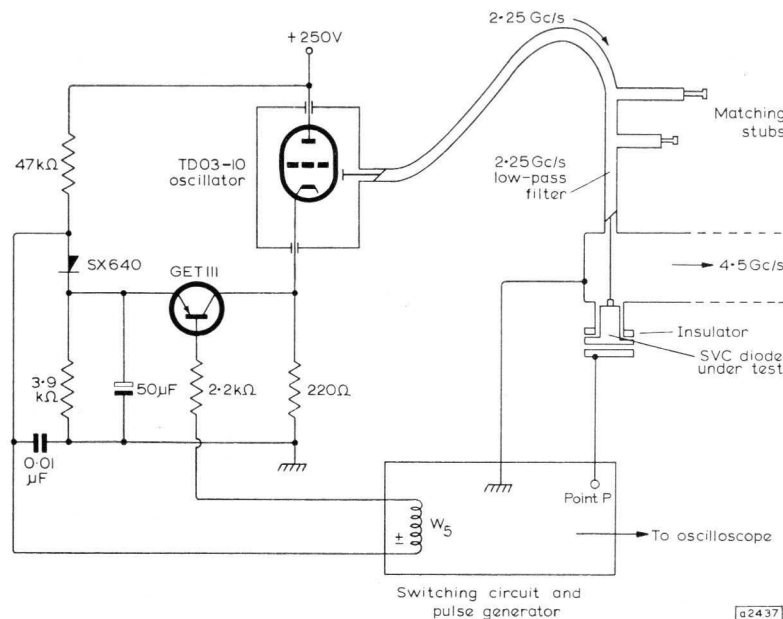


Fig. 6—Practical system



# Design of High-impedance Common-collector Input Stages

A. J. TUMBER

Mullard Semiconductor Measurement and Application Laboratory

The input impedance of a common-collector amplifier depends on the emitter load resistance, the gain of the transistor, and the shunt collector impedance. The effect of the shunt collector impedance can be minimised by operating at minimum emitter current and maximum collector voltage. It is shown that, with the OC202 transistor, an input impedance of at least 10MΩ (typically 25MΩ) in parallel with 28pF can be achieved.

## INTRODUCTION

The Mullard OC202 silicon transistor is known to have a useful value of current gain at low values of emitter current, suggesting that it could be used as a simple high input impedance amplifier. This article investigates its performance in the common-collector configuration. A typical input impedance of 25MΩ is achievable with the OC202. A considerable improvement on this figure is expected with transistors now in development.

## INPUT IMPEDANCE OF THE COMMON-COLLECTOR CONFIGURATION

### Derivation of Collector Shunt Impedance

We can see from a consideration of the hybrid-π equivalent circuit (Figs. 1 and 2, Ref. 1) that

$$Y_{IN} = \frac{1 - \alpha_0 + j\omega C_{b'e} r_e}{R_{eg}(1 + j\omega C_{b'e} r_e) + r_e} + \frac{1}{z_c} \quad \dots(1)$$

where  $R_{eg}$  is the parallel combination of  $R_E$  and  $r_{ce}$ , or

$$Z_{IN} = \frac{R_{eg}(1 + j\omega C_{b'e} r_e) + r_e}{1 - \alpha_0 + j\omega C_{b'e} r_e} \quad \dots(2)$$

in parallel with  $z_c$ , where  $z_c$  is  $r_{b'c}$  in parallel with  $C_{b'c}$ , which is

$$\frac{(1 + \beta)r_e}{\mu}$$

in parallel with  $C_{dep} + \mu C_{b'e}$ .

The derivation of Eq(1) is given in Appendix 1 (p. 178).

If we allow  $R_E$  to increase without limit, we shall obtain the shunt collector impedance of the common-collector configuration. Then

$$Z_{IN} = \frac{r_{ce}(1 + j\omega C_{b'e} r_e) + r_e}{1 - \alpha_0 + j\omega C_{b'e} r_e}$$

in parallel with  $z_c$ , from which we may deduce (Appendix 2, p. 178) that the collector shunt impedance is given by

$$r_{sh} = (1 + \beta) \cdot r_e / 2\mu \quad \dots(3)$$

in parallel with

$$C_{dep} + \mu C_{b'e}.$$

Substituting typical values from published data we obtain at  $V_{CE} = -6V$  and  $I_E = 1mA$

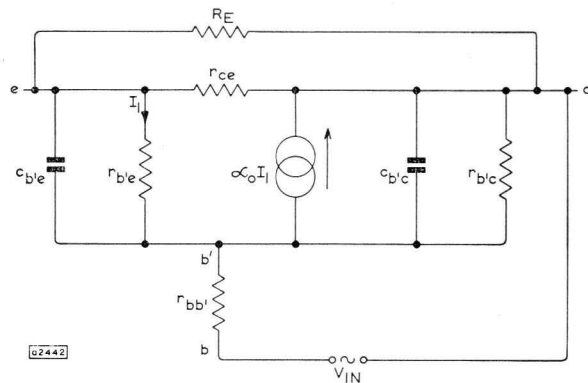


Fig. 1—Hybrid-π equivalent circuit in common-collector configuration

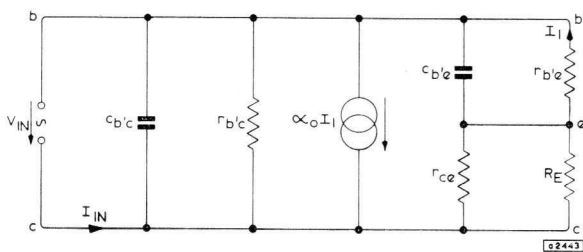


Fig. 2—Simplification of hybrid-π equivalent circuit

$$r_{sh} = \frac{71 \times 25}{2 \times 7.5 \times 10^{-4}} \approx 1.25M\Omega$$

and  $C_{sh} = 28 + 2000 \times 7.5 \times 10^{-4} pF = 29.5pF$ .

This is the impedance that occurs across  $(1 + \beta)R_E$  in the common-collector configuration and is valid (see Appendix 2) for

$$\omega \ll \frac{1 - \alpha_0}{C_{b'e} r_e} \quad \dots(4)$$

$$\ll \frac{1/71}{28 \times 10^{-12} \times 25} \ll 2 \times 10^7.$$

This condition will always apply, since the cut-off frequency is  $f$  where, with a typical source resistance of 100kΩ,

$$\frac{1}{2\pi f \times 29.5 \times 10^{-12}} = R = 100k\Omega \text{ in parallel with } 1.25M\Omega,$$

or

$$f = \frac{10^{12}}{2\pi \times 29.5 \times R} = 58kc/s.$$

**Variation of Shunt Impedance with Operating Conditions**

Let us examine the resistive part:

$$r_{sh} = \frac{(1+\beta)r_e}{2\mu} \dots (5)$$

Now  $r_e = AT/I_E$  and  $\mu = BT/\sqrt{V_c}$  (Ref. 2) where A and B are constants, T is the temperature in °K,  $I_E$  is measured in mA, and  $(1+\beta)$  is the current gain in the common-collector configuration.

The effect of reducing  $I_E$  is to increase  $r_{sh}$  over the range where the increase in  $r_e$  is proportionally greater than the decrease in  $\beta$ . Below a certain current the decrease in  $\beta$  predominates, and a maximum occurs at this point.

An increase in collector voltage will also increase  $r_{sh}$ , as both  $\beta$  and  $1/\mu$  will be greater.

The temperature coefficient of  $r_{sh}$  is that of  $\beta$ , since the quotient  $r_e/\mu$  is independent of temperature. The leakage current is exponential and doubles every 9°C, and  $\beta$  rises approximately linearly with temperature over the range 25 to 70°C.

Let us consider the effect of using a smaller emitter current, say 10µA.

Substituting into Eq(5), and using the published data typical values again, we have

$$r_{sh} = \frac{(1+\beta)r_e}{2\mu} = \frac{(1+20)2.5 \times 10^3}{2 \times 7.5 \times 10^{-4}} = 35M\Omega$$

and

$$C_{sh} \simeq C_{b'e} = C_{dep} + \mu C_{b'e} \simeq 28pF,$$

giving a bandwidth of 5.7kc/s with a source resistance of 1MΩ.

**EXPERIMENTAL DETERMINATION**

An attempt has been made to verify the above theory by measuring the incremental input resistance of the high-gain OC202 silicon transistor. The input resistance was obtained as a fraction of a known resistance  $R_B$  (see Fig. 3) from a measurement of the a.c. signal at the emitter. The input voltage and the voltage gain of the

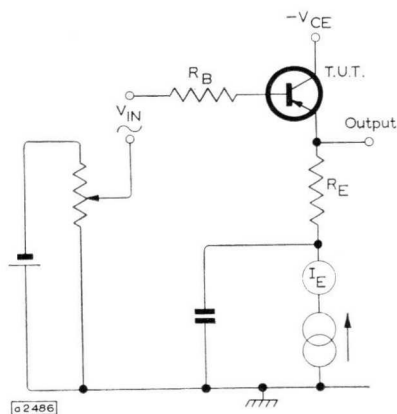


Fig. 3—  
Measuring circuit

transistor were known. In each series of measurements the input voltage was kept constant, and a separate determination of the voltage gain was made with a Tektronix differential input oscilloscope. The capacitor provides decoupling.

The value of  $R_E$  was varied from 100kΩ to 1MΩ, and measurements were made for  $V_{CE}$  from -2 to -10V and  $I_E$  from 10µA to 100µA. As the input resistance may be shown to be  $(1+\beta) R_E$  in parallel with the collector

shunt resistance  $r_{sh}$ , a graph of  $1/R_{IN}$  against  $1/R_E$  has a gradient of  $1/(1+\beta)$  and an intercept on the y-axis of  $1/r_{sh}$ . From a series of these graphs the variations of both  $\beta$  and  $r_{sh}$  with  $I_E$  and  $V_{CE}$  were determined.

To avoid inaccuracies as far as possible, the calculations and determination of  $\beta$  and  $r_{sh}$  were carried out by means of an Elliott 803 computer. The results obtained in this way are subject to an experimental error, as shown in Fig. 4.

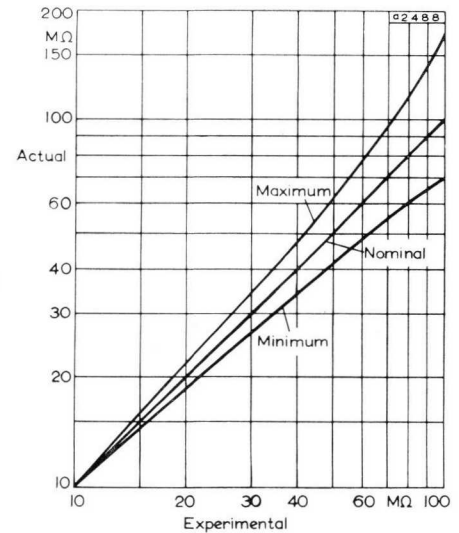


Fig. 4—  
Experimental accuracy

**CORRELATION OF THEORETICAL AND EXPERIMENTAL RESULTS**

**Absolute Magnitude**

The magnitude of  $(1+\beta)r_e/2\mu$  was calculated and compared with the experimental value. The calculation was based on measured values for  $\mu$ , a value of  $25/I_E$  mA for  $r_e$ , and the value obtained for  $\beta$  from the slope of the graph of  $I/R_E$ . A graph of experimental against calculated results (Fig. 5) shows that the values obtained experimentally differ slightly from those calculated,

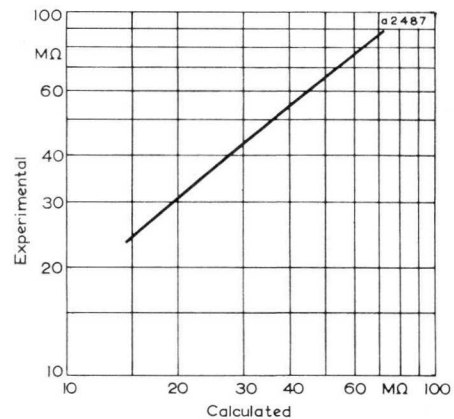


Fig. 5—Comparison of experimental and calculated values of  $(1+\beta)r_e/2\mu$

which indicates that the extrapolation of two orders of magnitude of the expression for  $r_e$  and  $\mu$  obtained at 1mA introduces some error. As the experimental results are higher than those calculated, this is of minor importance.

As will be seen in the following paragraphs, the variations of these parameters with emitter current, collector voltage, and temperature follow the theoretical analysis much more closely.

**Variation with  $I_E$**

The value of  $r_{sh}$ , calculated as above, was compared with the experimental result, and the variation of each with  $I_E$  was determined for several transistors. The comparative figures were obtained as follows:

Since the variation of  $\beta$  with current follows no simple rule and varies from one transistor to another, there is no exact expression for  $\beta/\beta_0$ ; but the approximation  $\beta/\beta_0 \approx (I/I_0)^n$  ... (6) applies over the current range 10 to 100  $\mu$ A. Since

$$\frac{r_e}{r_{e0}} = (I/I_0)^{-1}$$

the expression will be

$$r_{sh} = r_{sh(0)}(I/I_0)^m \dots (7)$$

where  $m = n - 1$ .

The mean value of  $m$  was determined from the variation of  $\beta$  with current found from the output graphs, giving the result  $-0.73$ . By experiment, the exponent has a mean value of  $-0.63$ . A typical graph of  $r_{sh}$  against  $I_E$  is shown in Fig. 6.

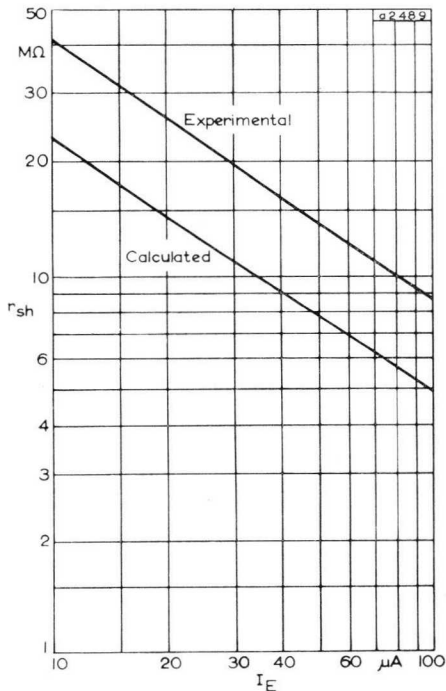


Fig. 6—Variation of  $r_{sh}$  with  $I_E$

Measurements of  $r_{sh}$  were carried out at lower currents in an attempt to find the value of  $I_E$  for which  $r_{sh}$  is a maximum. The voltage gain was found to fall rapidly below 5  $\mu$ A; so although the indications were that at this current  $r_{sh}$  was still increasing, the circuit is no longer useful.

**Variation with  $V_{CE}$**

A similar comparison was made between experimental and theoretical variations with collector voltage. On consideration of the effect of voltage on the parameters

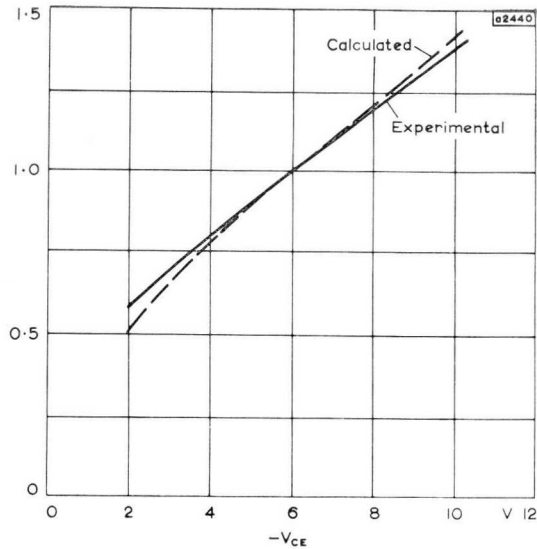


Fig. 7—Normalised variation of  $r_{sh}$  with  $V_{CE}$

in  $(1 + \beta) r_e / 2\mu$ , we find that  $\beta$  increases approximately linearly with increasing negative voltage at about 2.5% per volt of its value of  $-6V$ . The feedback factor  $\mu$  is inversely proportional to the square root of the magnitude of  $V_{CE}$ , and  $r_e$  is virtually independent of voltage.

From these relations, the variation about  $-6V$  may be calculated and expressed as a fraction of its  $-6V$  value. The ratios were similarly calculated, relative to the  $-6V$  figure, from the experimental results. The results are shown in Fig. 7.

**Variation with Temperature**

Both  $r_e$  and  $\mu$  are directly proportional to absolute temperature; and as these quantities occur as a quotient, the variation of  $(1 + \beta)r_e / 2\mu$  will be the same as that of  $(1 + \beta)$ . The two components  $(1 + \beta)R_E$  and  $(1 + \beta)r_e / 2\mu$  will therefore each change as  $(1 + \beta)$ ; and as  $R_{IN}$  is the parallel combination of these two, it will also change in this way.

The variation was measured with  $R_E = 100k\Omega$ ,  $I_E = 10\mu A$ , and  $V_{CE} = -6V$ . It was found that the incremental  $R_{IN}$  was directly proportional to temperature over the range 25° to 70°C, the variation being 0.6% of the 25°C value per degC (Fig. 8), compared with 0.5% measured for  $\beta$ . The change in current  $I_B$  due to the

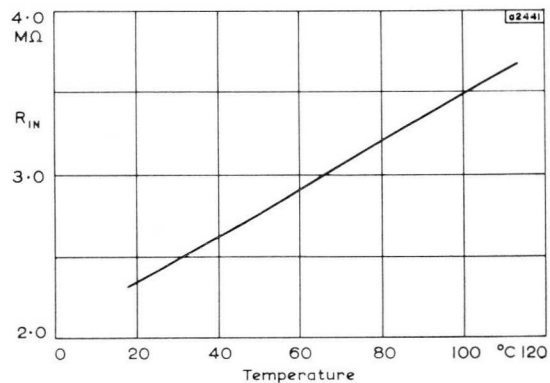


Fig. 8—Variation of  $R_{IN}$  with temperature

temperature change in  $\beta$  at  $I_E = 10\mu A$ , is of the same order (10nA) as the change in  $I_{co}$  at 25°C. At higher temperatures the leakage current predominates.

**SPREAD OF  $R_{IN}$  AT  $I_E = 10\mu A$**

The input resistance  $R_{IN}$  of the common-collector configuration is the parallel combination of  $(1+\beta)R_E$  with  $r_{sh}$ , where  $r_{sh} = (1+\beta)r_e/2\mu$ .

When the transistor production limits of  $\beta$  and  $\mu$  are taken into account, the value of  $r_{sh}$  may vary between 180MΩ and 6MΩ: a factor of 30. In practice, there is a correlation between  $\beta$  and  $\mu$  such that the transistor with a high value of  $\beta$  tends to have a high value of  $\mu$ , and vice versa, thus narrowing the spread of  $(1+\beta)/\mu$ . The value of  $r_{sh}$  is typically 35MΩ, and normally lies between 85MΩ and 14MΩ; a factor of 6.

If we have a minimum resistance transformation of 5, then  $R_E = R_{IN}/5$ , so that  $R_{IN}$  is given by  $(1+\beta)R_{IN}/5$  in parallel with  $r_{sh}$  (where  $\beta$  is subject to the full production spread, but, from the above considerations,  $r_{sh}$  is not).

If  $V_{CE}$  is increased from -6V to -12V, and the least favourable published values consistent with these reservations are substituted, then with the appropriate factors introduced to correct for the change in collector voltage,

$$R_{IN} = \frac{R_{IN}}{5} \quad (1+7) \times 1.15 \text{ in parallel with } 14 \times 1.6M\Omega$$

$$\frac{1}{R_{IN}} = \frac{0.55}{R_{IN}} + \frac{1}{23}$$

and

$$R_{IN} = 10.4M\Omega.$$

This is the minimum value of  $R_{IN}$  likely to be obtained, and is achieved with  $R_E = 2M\Omega$ . Here  $R_E$  is the parallel combination of the emitter resistance and the input resistance of the following stage.

With this same value of  $R_E$ , the value of  $R_{IN}$  that would be typically obtained at  $V_{CE} = -12V$  is given by:

$$R_{IN} = 2 \times (1+20) \times 1.15M\Omega \text{ in parallel with } 35 \times 1.6M\Omega = 48M\Omega \text{ in parallel with } 56M\Omega = 26M\Omega.$$

The maximum value of  $R_{IN}$  likely to be obtained with  $R_E = 2M\Omega$  is similarly given by

$$R_{IN} = 2 \times (1+40) \times 1.15M\Omega \text{ in parallel with } 85 \times 1.6M\Omega = 95M\Omega \text{ in parallel with } 140M\Omega = 56M\Omega.$$

**REFERENCES**

1. 'Mullard Reference Manual of Transistor Circuits', 2nd ed., 1961.
2. WOLFENDALE, E. 'The Junction Transistor and its Applications'. Heywood, 1958.

**APPENDIX 1**

**Input Conductance of Common-collector Configuration**

Consider the hybrid- $\pi$  equivalent circuit (Fig. 1). It may be rearranged as in Fig. 2; and, if the parallel combination of  $R_E$  with  $r_{ce}$  is denoted  $R_{eg}$ , we obtain

$$I_{IN} - V_{IN}/z_c + \alpha_0 I_1 = I_1(1 + j\omega C_{b'e}r_e)$$

or

$$I_{IN} - V_{IN}/z_c = I_1(1 - \alpha_0 + j\omega C_{b'e}r_e) \quad \dots(8)$$

and

$$V_{IN} = I_1 r_e + I_1(1 + j\omega C_{b'e}r_e)R_{eg} \quad \dots(9)$$

From Eqs (8) and (9)

$$(I_{IN} - V_{IN}/z_c)[(1 + j\omega C_{b'e}r_e)R_{eg} + r_e] = V_{IN}(1 - \alpha_0 + j\omega C_{b'e}r_e)$$

or

$$I_{IN}[(1 + j\omega C_{b'e}r_e)R_{eg} + r_e] = V_{IN}\{[1 - \alpha_0 + j\omega C_{b'e}r_e] + 1/z_c[(1 + j\omega C_{b'e}r_e)R_{eg} + r_e]\} \quad \dots(10)$$

giving

$$Y_{IN} = \frac{1 - \alpha_0 + j\omega C_{b'e}r_e}{R_{eg}(1 + j\omega C_{b'e}r_e) + r_e} + \frac{1}{z_c} \quad \dots(11)$$

**APPENDIX 2**

**Simplification of Expression for Shunt Collector Impedance**

$$Z_{IN} = \frac{r_{ce}(1 + j\omega C_{b'e}r_e) + r_e}{1 - \alpha_0 + j\omega C_{b'e}r_e} \quad \dots(12)$$

in parallel with  $z_c$ .

Rationalising the first term and neglecting  $r_e$  compared with  $r_{ce}$ , we obtain:

$$\frac{r_{ce}(1 + j\omega C_{b'e}r_e)(1 - \alpha_0 - j\omega C_{b'e}r_e)}{(1 - \alpha_0)^2 + \omega^2 C_{b'e}^2 r_e^2} \quad \dots(13)$$

or

$$\frac{r_{ce}(1 - \alpha_0 + \omega^2 C_{b'e}^2 r_e^2 - j\omega \alpha_0 C_{b'e} r_e)}{(1 - \alpha_0)^2 + \omega^2 C_{b'e}^2 r_e^2} \quad \dots(14)$$

If we restrict  $\omega \ll \frac{1 - \alpha_0}{C_{b'e} r_e}$  we have

$$\frac{r_{ce}(1 - \alpha_0 - j\omega \alpha_0 C_{b'e} r_e)}{(1 - \alpha_0)^2} \quad \dots(15)$$

of which the real part is:

$$\frac{r_{ce}}{1 - \alpha_0}$$

and the complex part is:

$$- \frac{j\omega \alpha_0 C_{b'e} r_e}{(1 - \alpha_0)^2}$$

This is the series form of the expression. The parallel equivalents are:

$$R_{parallel} = \frac{\left(\frac{r_{ce}}{1 - \alpha_0}\right)^2 + \left(\frac{\omega \alpha_0 C_{b'e} r_e}{1 - \alpha_0}\right)^2}{\frac{r_{ce}}{1 - \alpha_0}} \approx \frac{r_{ce}}{1 - \alpha_0} = (1 + \beta) \frac{r_e}{\mu} \quad \dots(16)$$

$$X_{parallel} = j \times \frac{\left(\frac{r_{ce}}{1 - \alpha_0}\right)^2 + \left(\frac{\omega \alpha_0 C_{b'e} r_e}{1 - \alpha_0}\right)^2}{-\frac{\omega \alpha_0 C_{b'e} r_e}{1 - \alpha_0}} \approx -j \times \frac{r_{ce}^2}{1 - \alpha_0} \cdot \frac{1}{\omega \alpha_0 C_{b'e} r_e} = \frac{r_{ce}^2}{j\omega(1 - \alpha_0)\alpha_0 C_{b'e} r_e} \quad \dots(17)$$

Therefore

$$C_{parallel} = \frac{(1 - \alpha_0)\alpha_0 C_{b'e} r_e}{r_{ce}^2} \quad \dots(18)$$

and, in combination with  $z_c$ , the collector shunt impedance is  $Z_{sh}$ , where

$$\text{Resistive part } r_{sh} \text{ is } \frac{(1 + \beta)r_e}{\mu} \text{ in parallel with } \frac{(1 + \beta)r_e}{\mu}$$

so that

$$r_{sh} = \frac{(1 + \beta)r_e}{2\mu}$$

$$\text{Reactive part } c_{sh} = c_{dep} + \mu C_{b'e} + \frac{(1 - \alpha_0)\alpha_0 C_{b'e} \mu^2}{r_e} \approx c_{dep} + \mu C_{b'e} \quad \dots(20)$$

The collector shunt impedance is  $\frac{(1 + \beta)r_e}{2\mu}$  in parallel with  $C_{dep} + \mu C_{b'e}$ .

# Dual Trace Oscilloscope Tubes

E. J. GRODSZINSKY

Mullard Applications Research Laboratory

*The characteristic features of double-gun cathode ray tubes and split-beam cathode ray tubes are described in this article. They are compared and contrasted in such a way as to assist circuit designers in choosing the more suitable kind of tube.*

## INTRODUCTION

It is often desirable to be able to display two independent waveforms simultaneously on the screen of one cathode ray tube, so that the traces can be interposed and their relationships studied. The two normal methods of accomplishing this, split-beam tubes and double-gun tubes, are discussed in this article in a way which is intended to assist oscilloscope circuit designers to choose the more suitable kind of tube for the particular application. Appendix I at the end of the article summarises the various characteristics of each type.

The two further methods often used to obtain twin traces are not discussed in this article since they do not display truly simultaneous waveforms. They are the use of beam-switching and the use of storage-tubes. Similarly the rare forms of simultaneous multi-trace oscillography, such as the optical combining of traces of several tubes, are not considered.

## Historical Background

It is worthwhile to consider briefly the development of the two methods being described. Since the c.r.t. is a complicated electronic device it was difficult to construct

double-beam tubes. These tubes had asymmetrical deflection and were used with a.c. coupled amplifiers. At this stage a few double-gun tubes had been constructed for special orders, but normal-scale production was impracticable.

About ten years ago the c.r.t. manufacturing technique was well enough established to allow the quantity production of double-gun tubes. The need for such tubes had been accentuated by the trend, at that time, towards the use of d.c. coupled amplifiers in oscilloscopes: the asymmetric deflection of the split-beam tubes then available made the use of single-ended amplifiers unavoidable and d.c. amplifiers in this form were unsatisfactory because of d.c. instability. In addition, a further objection to the asymmetric deflection system was the difficulty of obtaining sufficient deflection voltage, particularly at large bandwidths, from a single output valve rather than a 'push-pull' pair.

In the last few years split-beam tubes with symmetrical deflection have been designed and put into quantity production. These tubes overcome the drawbacks of the older asymmetric deflection tubes and, with the high ratios of post-deflection-acceleration now common, give satisfactory performance at higher bandwidth.

The two kinds of cathode ray tube with which the article is concerned are described below, and, later, the use of each in associated circuits is considered.

## DOUBLE-GUN TUBES

The double-gun cathode ray tube consists of a single glass envelope with two independent electron guns fitted in the neck. Some of the electrodes of the two guns may be interconnected inside the tube and a common post-deflection acceleration (p.d.a.) system and common screen are used. A schematic diagram of the electrode structure of this kind of tube is shown in Fig. 1.

Each electron gun may be constructed as a separate unit but the pairs are assembled as a rigidly aligned whole, with or without some electrical inter-connection, before being put into the envelope. An inter-gun shield (i.g.s.) is incorporated between the guns to shield them electrostatically from each other. A second screen, the outer gun shield (o.g.s.), may also be used both to assist in the screening between the two guns and to correct any electrostatic field distortion: adjustment of distortion in these tubes can be obtained by varying the potentials of these screens about the potential of the third anode.

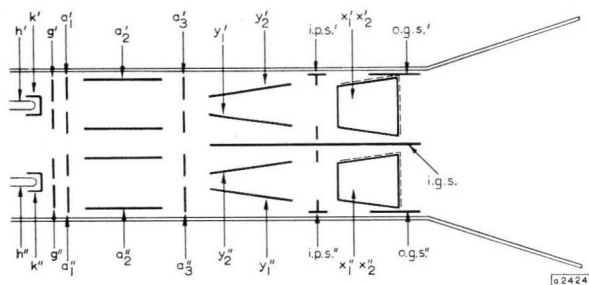


Fig. 1—Schematic diagram of double-gun tube

satisfactorily in its early days, and the guns in use were large. Consequently, the use of more than one gun was at first so difficult as to deter designers from attempting dual trace tubes.

The technique of beam-splitting was invented about twenty-five years ago, and led to the development of

There are problems which are specific to the design of these tubes. It is necessary to provide the best possible alignment of the traces in the x-direction by suitably arranging both the position of the beams and the angle between the beams. The sensitivities and the areas of scan should also be similar, particularly in the x-direction. Similar values of deflection-linearity about the centre are also required.

If a p.d.a. system is used, as is normal in present day tube types, then there is the additional problem that neither beam can pass symmetrically through the p.d.a. field. The distortion effects need to be carefully balanced in the tube design.

The two guns can be arranged either one on top of the other (Fig. 2a, b) or side-by-side (Fig. 2c). (In each case the y-axis is assumed to be vertical). The tube design with the guns placed one above the other is the most common: with this arrangement the y-plate capacitances are usually unbalanced. Complete y-scan overlap can be provided by an arrangement such as that shown in Fig. 2c, but rotated through 90°. With the horizontal layout of guns the first difficulty to be overcome in design is the alignment of the x-traces, a difficulty aggravated by the fact that the scan angle in the x-plane is normally greater than that in the y-plane. The x-plate capacitances may be unbalanced with this design because of the proximity of the x-plates to the screen, but such balance is not generally essential. The diagrams shown in Fig. 2 show the common arrangements of guns and the resulting 'windows'. Although the windows are similar, the arrangement shown in Fig. 2a presents the tube designer with the advantage of near-parallel guns, while the arrangement in Fig. 2b gives a beam symmetry which leaves less distortion to be countered by the designer.

The following points indicate the tube characteristics which are important to the circuit designer.

- (i) Each trace has independent brightness and focus control.
- (ii) It is generally possible to apply completely separate signals on both x- and y-plates, although with some tubes there are limitations on the frequency and voltage-difference permitted between the x-signals. In some tube designs, x-plates common to both guns are used.
- (iii) Provision must be made for the alignment and sensitivity equalisation of the two traces in the x-direction when a common timebase display is required, unless common x-plates are used.
- (iv) Problems associated with capacitive and field intermodulation exist with these tubes in the same way as with split-beam tubes. (See page 181).
- (v) The tube is inherently more complicated than the split-beam tube. In particular, since the tube has two guns, a fault occurring in either gun renders the tube faulty.

The list is by no means exhaustive but shows the main features which will affect basic circuit design.

**SPLIT-BEAM TUBES**

All modern split-beam tubes have symmetrical deflection systems; that is, they have a pair of y-plates for each beam, the pairs being separated by a shield. (The older split-beam tubes used asymmetrical deflection with only

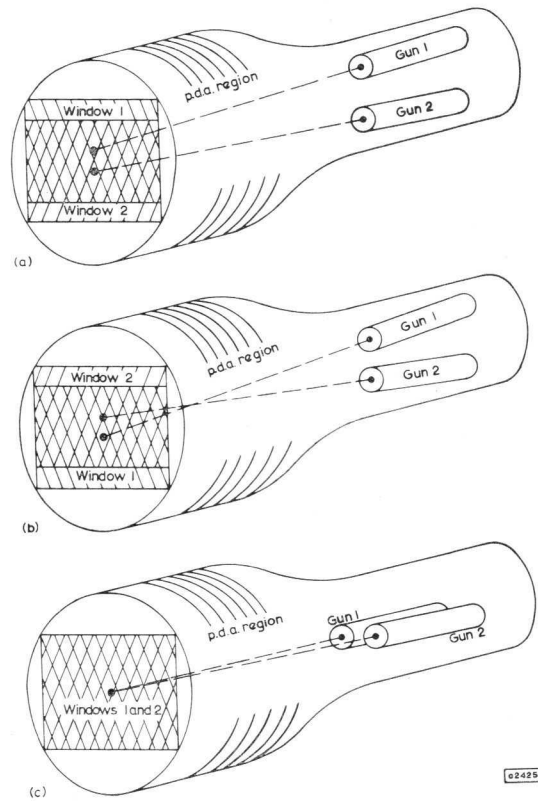


Fig. 2—Various positions for guns in double-gun tubes

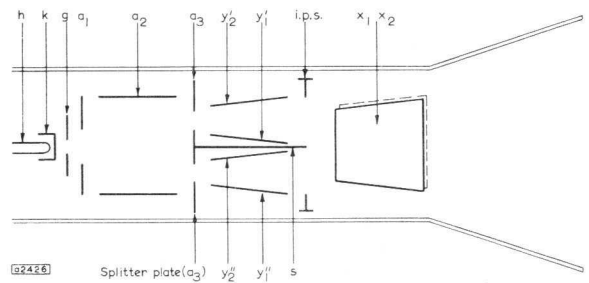


Fig. 3—Schematic diagram of split-beam tube

one independent y-plate for each beam and with the shield acting as a common y-plate between the beams.) The schematic diagram in Fig. 3 shows the electrode structure of a symmetrical deflection split-beam tube. The third anode is designed to act as a splitter-plate and both sections of the beam pass through independent y-plate deflection systems and then through a common x-plate system. Between the x- and y-plates is placed an inter-plate shield (i.p.s.) with a single slot for the two beams.

Many of the adjustment voltage-changes made in a tube of this kind must affect both beams. Thus, for example, adjustment of  $V_{a3}$  with respect to the y-plates for astigmatism correction, and adjustment of the i.p.s. voltage for raster correction, affect both beams. Brightness and focus adjustments are, of course, also common to both beams, although a special form of differential brightness control can be arranged by a method described on page 182.

The special characteristics of the split-beam tube are discussed below under appropriate headings.

#### Common X-deflection

The possibility of separate x-signals does not exist with split-beam tubes. Alignment of the traces in the x-direction is necessarily always exact at all parts of the screen, within the limits of any raster distortion. (This corresponds to perfect adjustment in a double-gun tube.)

#### Scan Areas

The x-scan areas overlap perfectly within the limits of any distortion, and when the beams are focused and pass undeflected through both y-systems then the spots coincide. The y-scan areas, however, do not overlap completely: there is a high proportion of common area, but each beam has, on its own side of the centre, an area into which the other beam cannot reach. This produces window areas similar to those shown in Fig. 2a and 2b for double-gun tubes.

#### Use of P.D.A.

The two traces are, in fact, parts of one beam originating in one gun. This is centralised in the p.d.a. system, and the separation between the beams in the p.d.a. region is small. Problems resulting from asymmetry are therefore minimised and the two deflection rasters are liable to suffer identically from any p.d.a. distortion, and any resulting asymmetry will be small and can be ignored. The normal undeflected beam lies on the axis of the tube, in contrast to the double-gun tubes shown in Fig. 2.

#### Unbalance of Y-capacitances

From the diagram in Fig. 3 it can be seen that the inner y-plates are placed very close to the shield, which is maintained at about earth potential. The capacitance of the inner plates to earth is therefore greater than that of the outer plates. The difference in capacitances amounts to only about 1pF in an effective push-pull y-plate capacitance of 6pF and this becomes even less significant when stray and valve output capacitances are added. The fact that the difference is so small is caused partly by the presence of further y-plate shielding surrounding the complete y-assembly.

#### Beam Current

It is common practice with instrument tubes to 'trim' the electron beam in either the first or third anode, or in both, so that only the core of the beam is used. With split-beam tubes the two apertures, placed as close to each other as the mechanical considerations of the y-assembly allow, effectively trim the beam but the core

centre is not used. The design of the splitter plate (a<sub>3</sub>) gives a compromise between light output, sensitivity and absence of deflection defocusing.

It is possible to have each aperture similar to that used in a single-gun tube. The dense core centre is not used and so the beam intensity is less than that for a single-gun tube. Each beam in a split-beam tube has about two-thirds of the density of the beam in a double-gun tube. In most present-day split-beam tubes, however, the excellent centre focus tends to allow the same maximum writing speed as is obtained with double-gun tubes at the same potentials.

#### Beam Equalising

With high beam currents the electron beam fills both apertures in the splitter-plate and if the apertures are identical in area then equal beam currents are obtained. When the beam current is lowered, however, the beam may not lie equally over the two apertures. To correct the resulting difference in beam brightness a small beam-equalising magnet is used, the poles of the magnet being placed near the control-grid region of the tube. By adjusting the strength of this field, across the aperture, the beam currents can be equalised for low values of beam current. The equalising is then maintained at the higher values of current.

#### Intermodulation

Intermodulation between deflection systems occurs in both split-beam tubes and in double-gun tubes. The main sources of intermodulation are capacitance, which gives an effect which is dependent on frequency if a resistive termination is used in the amplifier, and electrostatic fields, which give an effect independent of frequency, including d.c.

Capacitive intermodulation is to be discussed in a separate article issued later in this series. The discussion in that article will be based on the assumption that all modern tubes use symmetrical deflection in the y-direction and the x-direction. In all dual trace tubes it is possible to achieve a capacitive intermodulation figure as low as about 0.1% and by special circuit arrangements it can usually be reduced to zero.

Electrostatic field intermodulation is caused by the penetration of the electrostatic field due to one y-system into the volume controlled by the other y-system. Modern tubes provide an intermodulation figure, for this effect alone, of less than 0.1% with both kinds of tube.

Total intermodulation from both causes is usually less than one quarter of a line-width, when full screen deflection is applied to the other plates. This figure is normally quite acceptable.

#### Shift of Spot with Focus Adjustment

When the spots of a split-beam tube are defocused they also move in the y-direction. This is a disadvantage in setting up an oscilloscope but when focus is established and while it is maintained, the positions of the two traces are correct. The reason for the shift on defocusing is as follows. Undeflected focused beams in the split-beam tube

do in fact always coincide and appear as one spot, because the two beams are parts of one original beam. If therefore the focusing point of the beam is shifted along the beam-axis (the tube is defocused) then the two converging half-beams will strike the screen at different points giving separated spots. This is shown diagrammatically in Fig. 4 with a single-gun for comparison.

When a split-beam tube is defocused in an oscilloscope the y-positions of the two traces therefore move. As long as correct focus is maintained, then the accuracy of the readings from the y-trace is also maintained. The main problem lies in the fact that focus changes with drive (i.e. beam-intensity). This can always be corrected by refocusing, as would be necessary in any case before readings were taken.

**APPLICATION CONSIDERATIONS WITH BOTH TYPES OF TUBE**

When the two kinds of tube are being considered for a particular application then each tube offers some advantages and some disadvantages. A general point is that the split-beam tube is simpler than the double-gun tube and can be operated with less complex circuits: it therefore is often more suitable if a simpler kind of oscilloscope is planned. A second consideration which can be disposed of immediately is the possibility of requiring different x-timebases or x-expansions: only double-gun tubes can provide this, so that if it is necessary split-beam tubes are unsuitable. Other considerations are outlined below.

**Tube Electrode Supplies**

In all the previous comparisons the obvious underlying assumption is that the two types of tube are of similar size and operating potentials. If two such tubes are compared then generally it would be possible to operate the two tubes from identical power supplies, but twice the tube-gun current would have to be available for the double-gun tube. The p.d.a. supply current would be about the same in both cases. The heater power consumption would be doubled with two guns.

The controls for brightness, focus and astigmatism need to be duplicated for double-gun tubes. This provides operational freedom, but requires additional components and extra front-panel control space. In practice, as the writing speed and the occupance of both x-traces are the same, it seems unlikely that any normal arrangement would require different brightness settings.

Where differential brightness control is considered to be desirable it can be provided by using a controllable electromagnetic beam-steering magnet. (See Beam Equalising, page 181). The diagram shown in Fig. 5 indicates a possible structure and a method of connecting this into the circuit. Variations in  $RV_1$  permit variations of field strength from one polarity through zero to the opposite polarity. One difficulty with this system is that, as previously mentioned, variations in beam intensity may produce unwanted spot displacement, and excessive difference may produce spot distortion.

The only part of the gun-supply circuit which is normally dynamic in operation is the bright-up pulse circuit. When

this circuit uses grid or cathode modulation supplied from a bright-up amplifier the split-beam tube requires only one circuit. In the case of double-gun tubes two possible courses of action exist. Either separate amplifiers can be provided at extra cost, or both grids (or cathodes) can be driven by the same amplifier. Since a common gun supply has been assumed the latter course involves little difficulty but the amplifier does have to drive twice the grid (or cathode) capacitance. If, as is usual, a common bright-up amplifier is used with direct coupling, care must be taken in the design of the brightness control circuit as the two guns may have a spread in 'cut-off'

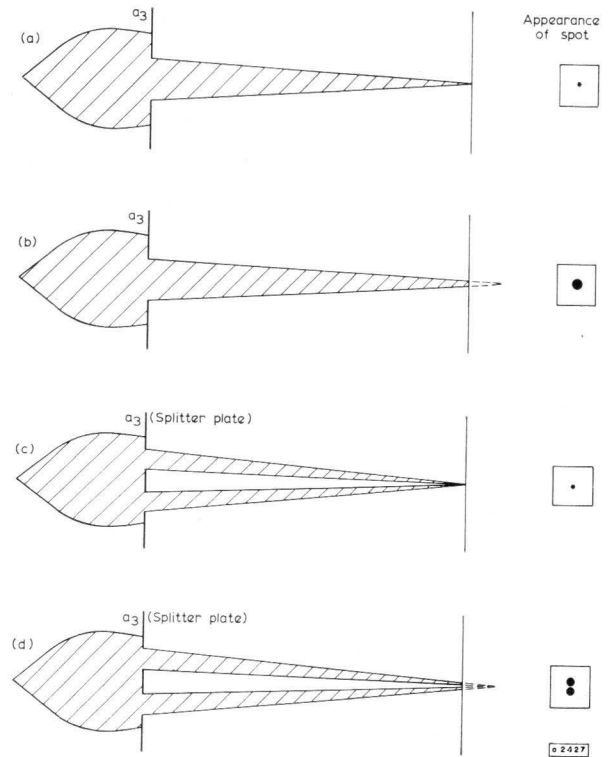


Fig. 4—Defocusing in c.r.t. The diagrams in (a) and (b) show defocusing with a single beam. The diagrams in (c) and (d) show how spot-shift occurs with a defocused split-beam

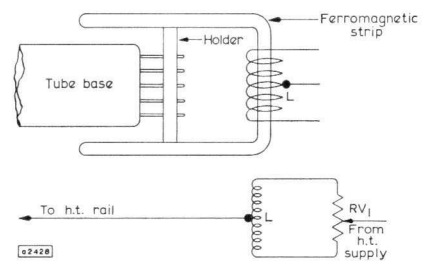


Fig. 5—Method of obtaining differential brightness with a split-beam tube

characteristics. The most convenient solution to the problem is usually either to apply the bright-up pulse to the grids and the brightness controls to the cathodes, or vice versa.

If there is a considerable difference in the cut-off voltage of the two guns the writing speeds of the two traces



APPENDIX 1

The preceding article compares split-beam tubes and double-gun tubes, and is intended to assist circuit designers to select tubes suitable for a particular application. The characteristics of each kind of tube are tabulated below.

may differ slightly if the same bright-up pulse is applied. This difficulty does not occur with a split-beam tube using some form of beam equalising.

If a deflection-blanking system is used, some of the above points will not arise, but the bright-up circuit must feed into twice the capacitance as these are two guns, and the voltage on the first anode must be unaltered. It is hoped to discuss the problem of deflection blanking in a later article.

**X-deflection Circuits**

Only the completely common x-deflection arrangement is considered in this comparison of circuits. Three main conditions need to be satisfied in the final oscilloscope. They are, equal x-deflection sensitivity, correct positioning of the two spots and correct x-tracking. These requirements are provided for in the split-beam tube, but special precautions are necessary in the double-gun tube.

Sensitivity and spot-position for the two guns can be adjusted to some extent in the circuit by pre-set alignment controls. Tracking accuracy will be obtained provided that equally linear voltages are applied to the x-systems.

With the assumed common x-deflection the split-beam tube retains all the advantages with fewer disadvantages. When the necessary adjustments are provided for the double-gun tube (using common x-deflection), there is an increase in the number of circuit components, in the assembly time and in test time. If the double-gun tube is used with a single amplifier to drive both x-deflection systems then the amplifier will need to be comparatively large to drive the double capacitance and the associated adjustment circuit. A double-gun tube with a single pair of x-plates avoids such problems. The capacitance of such a large x-plate system would be somewhat greater, and the tube would lose its versatility in other applications while retaining the complications of a two-gun structure.

**Y-deflection Circuits**

The general requirements of the y-deflection systems are similar for split-beam and double-gun tubes. Conventional long-tailed-pair amplifiers are generally used and the control arrangements and performance expected would be similar.

The split-beam tube is, however, generally designed in such a way that the resulting y-sensitivity is only about 70% of that for a comparable double-gun tube. Capacitances and intermodulation in the two kinds of tube are of the same order. The maximum bandwidth obtainable, therefore, with a particular valve line-up will be somewhat less with split-beam tubes.

In the case of split-beam tubes the mean y-potentials of the two y-systems must be similar since only one astigmatism control voltage can be applied when  $V_{a3}$  is used for this adjustment. These mean potentials are, in any case, likely to be identical, when identical y-plate amplifiers are used.

Circuits of some y-plate amplifiers for split-beam tubes are to be discussed in a later article.

**Performance**

These notes assume optimum gun designs and similar operating conditions in tubes of the same size. (All figures are approximate.)

Characteristic	Split-beam Tube	Double-gun Tube
Heater Wattage	P	2×P
Focus Quality (see Note 1)	No essential difference	
Spot Movement with Focus	Present	Absent
Beam Current (Typical—each trace)	I	1.5×I
Max. Writing Speed (see Note 1)	S	1.5×S
X-total Scan Volts (Volts to scan window)	X	X
X-alignment (angular)	0°	within 1°
X-tracking	Perfect	Good
X-scan Size	Full Screen	Full Screen
X-overlap	Complete	Complete
X-capacitance (effective) (see Note 2)	C (both traces)	C (each trace)
Y-total scan volts (volts to scan window)	Y	0.7×Y
Y-alignment (angular)	Within 1°	Within 1°
Y-scan height (typical for 4in tube)	5cm	5cm
Y-scan overlap (typical for 4in tube)	4cm	4cm
Y-capacitance (effective)	C	0.9×C
Y-intermodulation, capacitive	≤0.1%	≤0.1%
Y-intermodulation, field	≤0.1%	≤0.1%
Permissible max. Y'-Y'' mean plate potential difference	Small	Larger
Max. P.D.A. Ratio (typical) (see Note 3)	4 : 1	4 : 1
<b>Controls</b>		
Brightness	One	Two
Focus	One	Two
Astigmatism (see Note 4)	One	Two
X-sensitivity – balance	None	Required
X-position adjustment	None	Required
Y-deflection system controls	Con-ventional	Con-ventional

Notes

1. The compromise between design factors in the case of existing tubes gives smaller spot sizes in split beam tubes. Writing speeds are therefore almost equal.
2. If common x plates are used in the double-gun this figure may then be about 1.5×C for both traces.
3. Figures are quoted on existing tube types. The split-beam tube is more suitable for higher p.d.a. ratios, as the beams are nearly coaxial with the tube. This would allow sensitivity improvement for a given writing speed.
4. It is possible to arrange two astigmatism controls in the split-beam tube, although it is not necessary.

# Trigger Tube Coupling Circuits for Counting Tubes

G. F. JEYNES and S. ZILKHA

Mullard Applications Research Laboratory

*The interstage coupling in a chain of cold-cathode counting tubes can take various forms—valve, cold-cathode tube, and transistor circuits being possible. In the present article, cold-cathode trigger tube coupling circuits for operation at 0 to 40c/s and 0 to 400c/s are described, with design considerations, auxiliary circuits for power supply and resetting, and performance figures.*

## INTRODUCTION

When decade counting tubes are used in a series chain, to give an indication representing two or more significant figures, provision must be made for coupling the output from one counting tube to the input of the next. By this means, the 'units' counter passes a signal, after each count of ten, to the 'tens' counter, and so on. The coupling circuit can be designed round valves (Ref. 1), cold cathode tubes (as in the present article), or transistors.

In this article a coupling circuit for operation at a maximum frequency of 40c/s is described, and also a variant which has a maximum of 400c/s. These circuits can be used in conjunction with the Z504S decade counting tube for counting at a maximum rate of 4kc/s. The system is shown schematically in Fig. 1.

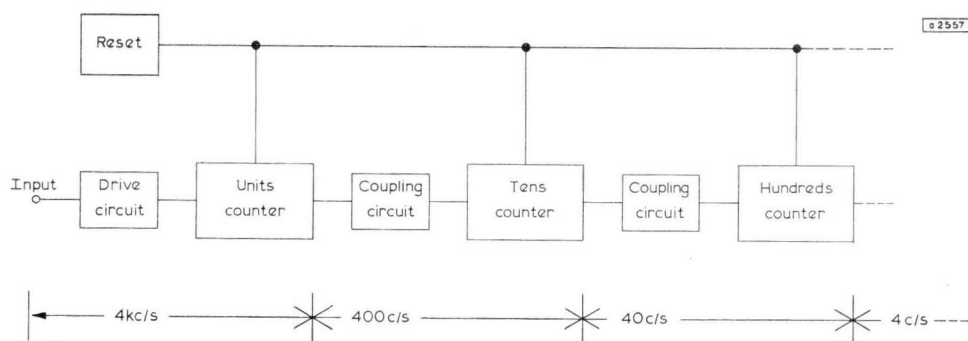


Fig. 1—Counter chain

The article includes details of a power supply unit that provides the required voltage rails in an economical manner. A circuit for resetting the counter to zero is also given. A detailed article on the design of resetting circuits will be published shortly.

## DESIGN REQUIREMENTS

The design of a coupling circuit for a counter tube chain is determined largely by the characteristics of the counter tubes. The circuit must be capable of operating from the pulse available from the output of the first

counter tube; it must itself provide an output pulse that is suitable for driving the second counter tube; and it must operate at the required frequency.

## Frequency Considerations

The Mullard decade counter tube type Z504S has a maximum operating frequency of 5kc/s. For a counter chain in which the tube is to be operated from an un-stabilised anode supply, and with mains voltage fluctuations and component tolerances, a maximum operating frequency of 4kc/s is recommended.

The coupling circuit which follows the first decade tube must, therefore, be capable of operating at  $4000/10 = 400\text{c/s}$ . The subsequent coupling circuits will then have maximum operating frequencies of 40c/s, 4c/s, 0.4c/s . . . . It is convenient, in practice, to design a high-speed coupling circuit for the 400c/s stage, and a low-speed circuit which will be suitable for all the stages operating at 40c/s or lower frequencies.

## Input Drive to Z504S

The coupling circuit must provide a pulse to drive guide A of the following Z504S, and a delayed pulse to drive

guide B. Each pulse must have a duration of at least  $60\mu\text{s}$  on each guide, and a negative pulse excursion of at least 45V with respect to the cathode — either a main or guide cathode — on which the discharge rests.

The choice of guide bias is a compromise. With a high guide bias there is a deterioration in life performance; but on the other hand a low guide bias leads indirectly to a decrease in the amplitude of the output pulse. The lower limit is dictated by the need to limit the maximum positive excursion of the output cathode voltage to 10V below the guide bias level. This provides a safety margin against

differences in the Z504S cathode maintaining voltages in the region of the output cathode. A positive bias level of 40V has been chosen as a suitable compromise.

The guide pulse is the sum of the positive guide bias and the negative voltage excursion at the guide cathodes.

The Z504S has a maximum voltage limit of 140V between any two main or guide cathodes, set by possible spurious breakdown within the tube.

**Output Pulse from Z504S**

When the discharge in the Z504S transfers from  $k_9$  to the output cathode  $k_0$ , the output pulse generated must be capable of driving the coupling stage under all operating conditions. This output pulse is the sum of the negative bias and the maximum positive potential that  $k_0$  is permitted to go to.

The absolute maximum permitted value of negative bias is -20V. For very long life, and with an unstabilised negative bias supply, a nominal bias of -12V is chosen. With the recommended positive bias of 40V on the guide cathodes, the output cathode, as mentioned earlier, has a permitted positive excursion of 30V; therefore the output pulse from  $k_0$  has a nominal amplitude of  $30 + 12 = 42V$ . This amplitude may vary by  $\pm 24\%$ , if the output circuit consists of a single resistor, if mains variations of  $+10\%$  and  $-15\%$  and resistor tolerances of  $\pm 7\%$  are encountered, and with allowance made for the Z504S maintaining voltage range. The variation of pulse amplitude may, however, be held within  $\pm 5\%$  by the inclusion of a diode in the output circuit, as described on page 186.

**TRIGGER TUBE COUPLING CIRCUITS**

In the present article, two coupling circuits which use cold-cathode trigger tubes are described.

The ideal requirements of the coupling circuit are that it shall be designed to return to its original condition immediately after each pulse; that, for economy, it shall require only one trigger tube; that it shall run off the

same supplies as the counter tubes; and that the supplies shall be unstabilised. The first two requirements can be met; but the characteristics of the available types of trigger tube necessitate some elaboration of the voltage supplies. Thus, the Mullard Z700U trigger tube, which is used in the two practical circuits, requires an anode voltage supply of 270V, whereas the Z504S counter tube operates from a 525V supply. And the need to allow for life variations in the Z700U, requires stabilisation of some of the voltage rails for the coupling circuit. However, these supply requirements can be met economically.

The Z700U has been used in the coupling circuit because its short recovery time permits operating speeds in excess of 400c/s. In addition, this tube has the advantages of small physical size and low cost. A self-extinguishing circuit has been used to take advantage of the large pulse generated at the anode as the tube fires, and thus to obtain the large-amplitude pulse required to drive the guide cathodes.

**LOW-SPEED COUPLING CIRCUIT**

A simplified form of the basic 0 to 40c/s coupling circuit is shown in Fig. 2. The coupling stage consists of a Z700U cold-cathode trigger tube  $V_2$  in a self-extinguishing circuit.

The output pulse at  $k_0$ , the output cathode of the first stage  $V_1$ , is fed via  $C_1$  to the prebiased trigger of the Z700U. The prebias is applied via  $R_3$ .

The anode self-extinguishing circuit comprises the anode resistor  $R_4$  and capacitor  $C_2$ . The output pulse of the Z700U is fed through the coupling capacitor  $C_3$  to the pulse-shaping network. The potential divider  $R_5$  and  $R_6$  applies the required pulse to the guide A cathodes of the succeeding stage  $V_3$ , and the integrator network  $R_7$  and  $C_4$  applies a delayed pulse to the guide B cathodes. Resistor  $R_6$  supplies positive guide bias to guides A and B.

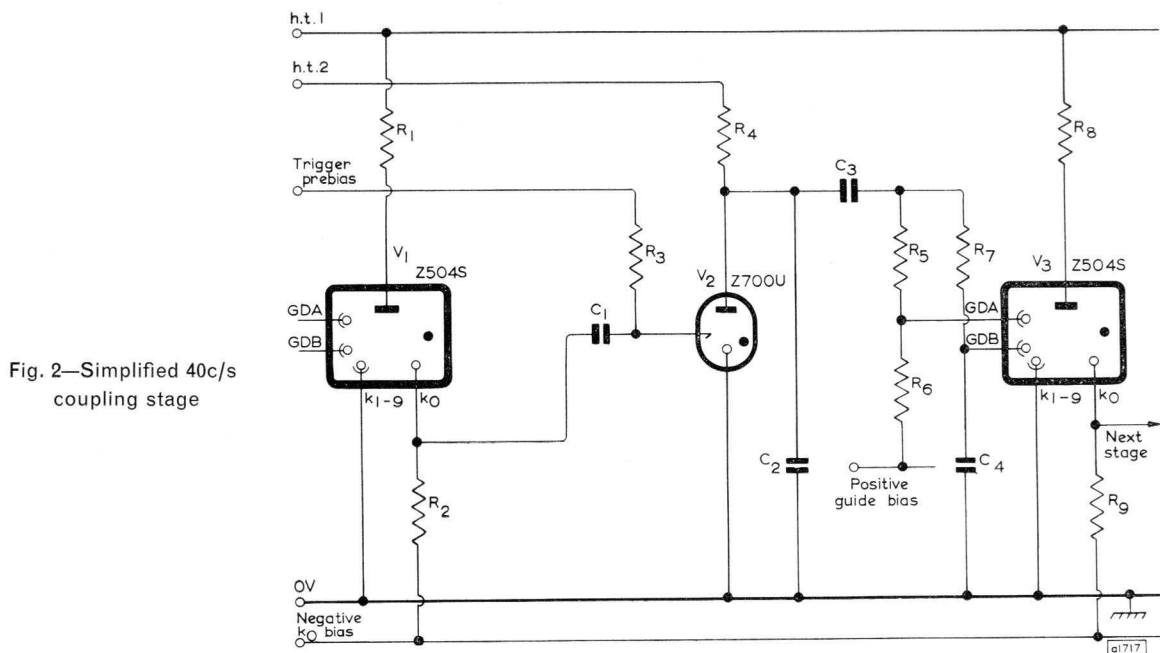


Fig. 2—Simplified 40c/s coupling stage

**Drive Pulses to Second Counter**

As the trigger tube fires, capacitor  $C_2$  discharges rapidly through the tube, and a large pulse is produced at the anode of the Z700U. The tube then extinguishes, and its anode potential returns exponentially to the h.t. supply level with a time-constant largely determined by  $R_4C_2$ , as shown by  $V_S$  in Fig. 3. The network  $R_7C_4$

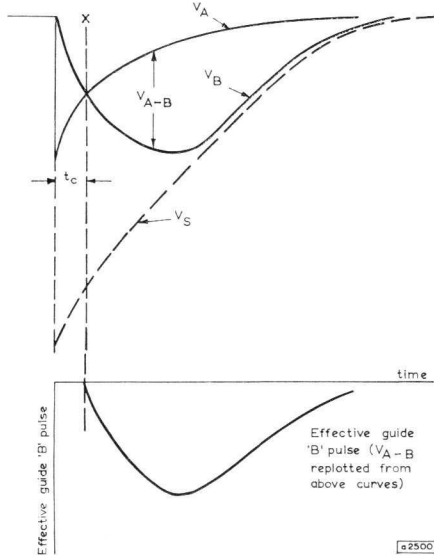


Fig. 3—Drive pulse and guide A and B waveforms

integrates this pulse, as shown by  $V_B$ , and this waveform is applied to the guide B cathodes. It will be seen that at no time can the guide B voltage become more negative than  $V_S$ , so that if  $V_S$  is applied directly to the guide A cathodes, the discharge cannot transfer from a guide A to a guide B cathode. However, with  $V_S$  attenuated by the resistive potential divider  $R_5R_6$ , an attenuated waveform (shown by  $V_A$  in Fig. 3) is applied to the guide A cathodes,

whilst the guide B waveform remains unchanged. The discharge may now transfer from a guide A cathode to an adjacent guide B cathode as soon as the guide B voltage becomes more negative than guide A.

Transfer to guide B will occur after the crossover point 'X' is reached, so that the interval  $t_c$  represents the theoretical minimum rest period on the guide A cathodes. In practice, the rest period on guide A is always greater than  $t_c$ , since the guide B cathodes must become substantially negative compared with the guide A cathodes before the discharge transfers. This voltage difference, which constitutes the effective guide B negative pulse, must exceed 45V for satisfactory operation, and is indicated by  $V_{A-B}$  in Fig. 3. A typical voltage difference curve is shown separately in Fig. 3.

**Output Pulse from First Counter**

The greatest nominal output pulse excursion permitted by the stepping tube is from  $-12V$  to  $+30V$ ; that is, a nominal 42V pulse. The most simple output circuit consists of a single  $k_0$  resistor  $R_2$ . However, this simple arrangement cannot be employed here, because of the relatively large variations in output voltage caused by component tolerances and supply voltage fluctuations. Instead, a large output cathode resistor  $R_2$  is used in conjunction with a clamping diode  $D_1$  returned to a positive 30V supply, as shown in the practical circuit, Fig. 4.

The tolerance on the positive excursion of the output pulse is now fully defined by the clamp voltage tolerance rather than by the wider variations in stepping tube current. If we assume a  $\pm 10\%$  variation in the clamp voltage (consisting of 5% supply variations and 5% potential divider drift) and a 15% variation in the  $k_0$  bias voltage, a minimum output pulse of 38V is generated.

The value of  $R_2$  in Fig. 4 must be high enough to ensure that most of the  $k_0$  output current is available to trigger the Z700U; but a maximum limit is set by the voltage

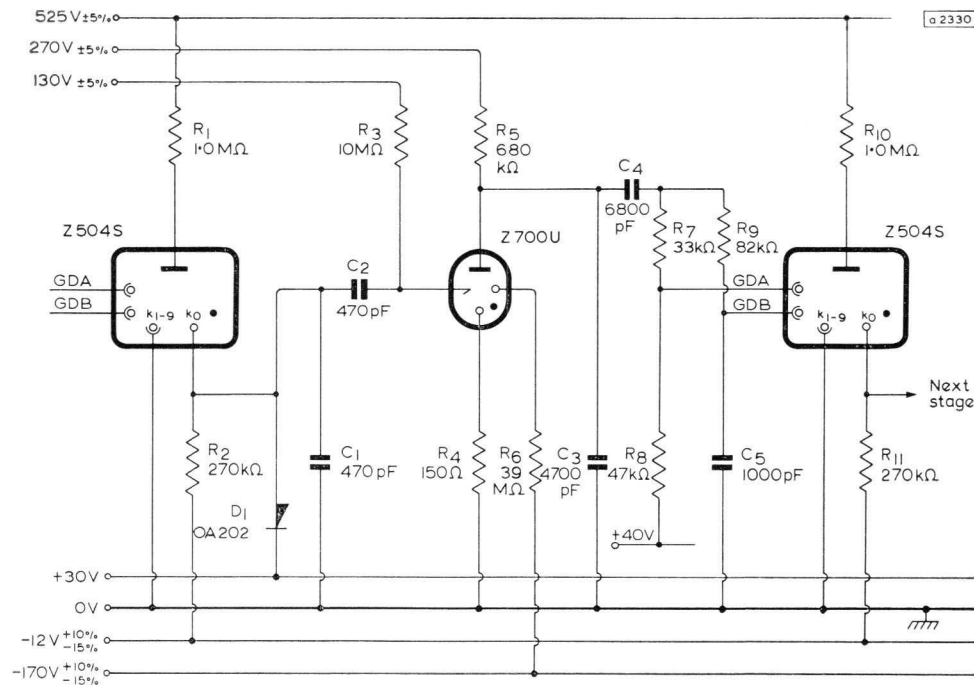


Fig. 4—Practical 40c/s coupling stage  
 $R_1, R_7, R_8, R_9, R_{10}$  are  $\frac{1}{4}W, \pm 7\%$  total excursion  
 $R_2, R_3, R_4, R_5, R_6, R_{11}$  are  $\frac{1}{4}W, \pm 10\%$   
 All capacitors are  $\pm 10\%$

developed by cathode leakage current which may flow when the discharge is not resting on  $k_0$ .

The published trigger ignition voltage range for a Z700U is from 137V to 153V. For calculation, an extended range of 137V to 160V has been adopted to give an additional margin of safety and an overvoltage for rapid ionisation of the tube. Under the worst-case limit conditions, with a minimum output of 38V applied to a tube with a maximum ignition voltage of 160V, a prebias of at least 122V is necessary to ensure firing of the Z700U. As the maximum permitted prebias which may be applied without firing the tube, in the absence of a  $k_0$  output pulse, is 137V, satisfactory operation under all circuit conditions is obtained with a prebias supply of  $130V \pm 5\%$ .

The values of  $R_3$  and  $C_2$  (Fig. 4) must ensure self-extinction of the Z700U, and must provide a time-constant short enough to allow full recovery of the trigger circuit. At an operating frequency of 40c/s, the available recovery time between successive input pulses is 25ms. The value of  $R_3$  must exceed  $700k\Omega$  to ensure extinction. Use of a value of  $10M\Omega$  will minimise the capacitive loading of  $C_2$  on  $k_0$  and will also keep down the cost of  $C_2$ .

#### Prevention of Spurious Firing

Capacitor  $C_1$  has been added to ensure that the trigger circuit does not fire spuriously at the end of the input pulse.

Consider the circuit when  $C_1$  is not included. As the discharge transfers to  $k_0$ , a 42V pulse is applied to the trigger of the Z700U, and the tube fires. The anode capacitor then discharges, and the anode voltage falls below its maintaining value, so that the tube extinguishes.

In the present instance the anode voltage falls to about +60V in a conduction period of about  $20\mu s$ . As it does so, it pulls the trigger voltage down to a similar level. Thus, a negative voltage step of about 110V appears at the trigger, causing the voltage at  $k_0$  to fall by 90V from +30V to -60V. (The 20V reduction of the voltage step is caused by the flow of current through  $C_2$  from  $k_0$  during the conduction period.)

Now, as the Z700U extinguishes, the  $k_0$  current rapidly charges the stray capacitances in the circuit, and returns  $k_0$  to +30V, thus generating a positive 90V step which causes the trigger to rise from +60V to about +150V. As this voltage is greater than the minimum ignition voltage for the Z700U, some tubes may fire again, and a spurious pulse will appear at the output.

When  $C_1$  is added,  $C_1$  and  $C_2$  act as a capacitive potential divider. With  $C_1 = C_2$ , only half the initial voltage step is fed back to  $k_0$ . Thus, when the tube extinguishes, a smaller positive pulse is applied to the trigger, followed by a slow rise to the prebias level. Capacitor  $C_1$  is charged by the flow of  $k_0$  current in approximately  $100\mu s$ . Capacitor  $C_2$ , however, charges with a time-constant  $R_3C_2 = 4.7ms$ . Under these conditions, the tube cannot re-fire. The addition of  $C_1$  causes no measurable reduction in the amplitude of the pulse applied to the trigger of the Z700U.

#### Guide Pulse Shaping

The output circuit of the Z700U shapes the drive pulses for the Z504S. The values of the circuit components are

very interdependent, and the determination of values will not be described in detail. However, as an aid to the designer, a number of design criteria are given.

When the Z700U fires, its anode voltage falls from the h.t. level to about 60V as  $C_3$  discharges through the tube and the current-limiting resistor  $R_4$ . This step defines the output pulse. The guide A pulse amplitude is determined by the ratio between  $R_7$  and  $R_8$ . Ideally, as much output energy as possible should be transferred from the Z700U to the pulse-shaping network. Both  $R_7$  and  $R_8$  should therefore be large to avoid charging  $C_4$  unnecessarily. However, the sum of  $R_7$ ,  $R_8$ , and  $R_9$  should be below  $200k\Omega$ , so that when the discharge is quiescent on a main cathode, the leakage current will not cause the guides to rise above 42V. If they do, a short standby life may result. The guide A pulse amplitude is, in practice, slightly smaller than the calculated value because of the flow of guide A current through the effective impedance of the potential divider  $R_7$ ,  $R_8$ .

The amplitude of the effective guide B pulse is determined by the difference between the guide voltage waveforms after the crossover point 'X' in Fig. 3. The amplitude depends on the amplitude of the pulse appearing at the junction of  $C_4$  and  $R_7$  in Fig. 4, and also on the integrator circuit time-constant  $R_9C_5$ .

The recovery time of the anode waveform contains two time-constants. Firstly, a rapid charging of  $C_3$  by current flowing via  $R_5$  largely determines the period for which the discharge rests on the guide A cathodes. Secondly, a slower charging of  $C_4$  via  $R_5$ ,  $R_7$ , and  $R_8$  determines the total recovery time of the circuit.

The time-constant of the rise of Z700U anode voltage must be greater than  $150\mu s$  for self-extinguishing operation. However, this time-constant is too short to allow a satisfactory period of rest on the guide A cathodes. The time-constants have been chosen to give satisfactory periods of rest on the guide A and guide B cathodes, which then allow the circuit to recover within 25ms, thus providing a maximum operating frequency of 40c/s.

#### Performance of 40c/s Circuit

Fig. 5 shows the guide A and B voltage waveforms with both guide circuits connected, again at nominal supply conditions. It can be seen that, typically, the guide B cathodes become about 15V negative with respect to the guide A cathodes before the discharge transfers to

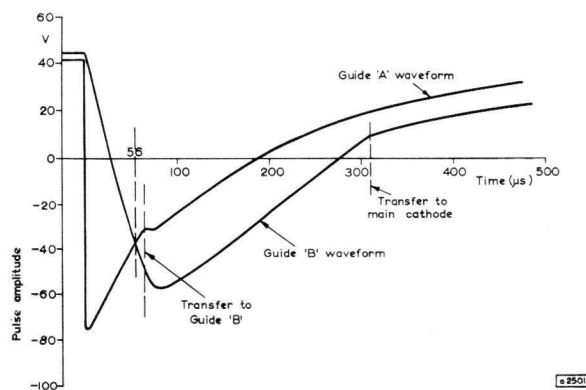


Fig. 5—Observed guide A and B waveforms (40c/s circuit)

guide B. It will also be seen that the guide B bias is slightly greater than the guide A bias, because of probe-current flow through  $R_7$  and  $R_9$ .

Measured performance figures for the 0 to 40c/s circuit are given in Table 1 for nominal conditions and for two worst-case conditions.

The minimum period of rest on the Z504S guide A cathodes is  $56\mu\text{s}$ , which is below the rated minimum of  $60\mu\text{s}$ . Extensive life tests have shown, however, that for this application the extension of the limit is acceptable on condition that the period of rest on the guide B cathodes does not fall below  $100\mu\text{s}$ .

TABLE 1  
Performance of 0 to 40c/s Circuit

	SUPPLY VOLTAGES			
	Min.*	Nominal**	Max.†	
<b>Guide 'A'</b>				
Pulse amplitude	108	115	124	V
Typical period of rest	70	70	70	$\mu\text{s}$
Time for full recovery	800	900	800	$\mu\text{s}$
<b>Guide 'B'</b>				
Pulse amplitude	88	100	105	V
Typical period of rest	245	255	245	$\mu\text{s}$
Time for full recovery	1000	1200	1200	$\mu\text{s}$
Time to crossover	56	56	56	$\mu\text{s}$

\*Positive supplies  $-5\%$ , negative supplies  $-15\%$ , frequency 40c/s.

\*\*Positive and negative supplies nominal, frequency 40c/s.

†Positive supplies  $+5\%$ , negative supplies  $+10\%$ , frequency 10c/s.

The values quoted will vary by  $\pm 5\%$  from one sample of Z700U to another, because of variations in the anode extinction voltage.

ADAPTATION FOR 400c/s OPERATION

The 0 to 40c/s circuit can be adapted for operation at frequencies up to 400c/s by adjustment of component values, increase of the voltage available for recharging  $C_4$  during recovery, and the addition of two diodes.

The main differences are dictated by the need to shorten the circuit recovery time, since the period available is obviously reduced with the increased operating frequency.

Fig. 6 shows the complete 0 to 400c/s circuit.

Trigger Circuit

The trigger circuit time-constant  $C_1R_3$  (Fig. 6) has been reduced to  $560\mu\text{s}$  for full recovery at 400c/s. Capacitor  $C_2$  has been reduced to keep the rise-time of the  $k_0$  output voltage to a fraction of the trigger circuit time-constant. However,  $C_2$  is still large enough to act, in conjunction with  $C_1$ , as a capacitive potential divider to limit the pulse fed back to  $k_0$  when the Z700U fires. The trigger voltage available for firing the Z700U is slightly less than in the low-speed circuit; but it is still sufficient for operation under all circuit conditions.

With a ten to one reduction in trigger circuit time-constant, the rise-time of the output pulse from the previous Z504S must be short if the pulse available for triggering the Z700U is not to be attenuated. In many cases the rate of rise of the  $k_0$  output voltage can be determined by the trailing edge of the guide B waveform. The discharge in the Z504S transfers to the output cathode when the guide B voltage has risen to about zero volts; that is, when the output cathode is 12V negative compared with the discharge on guide B. As the discharge is formed, the

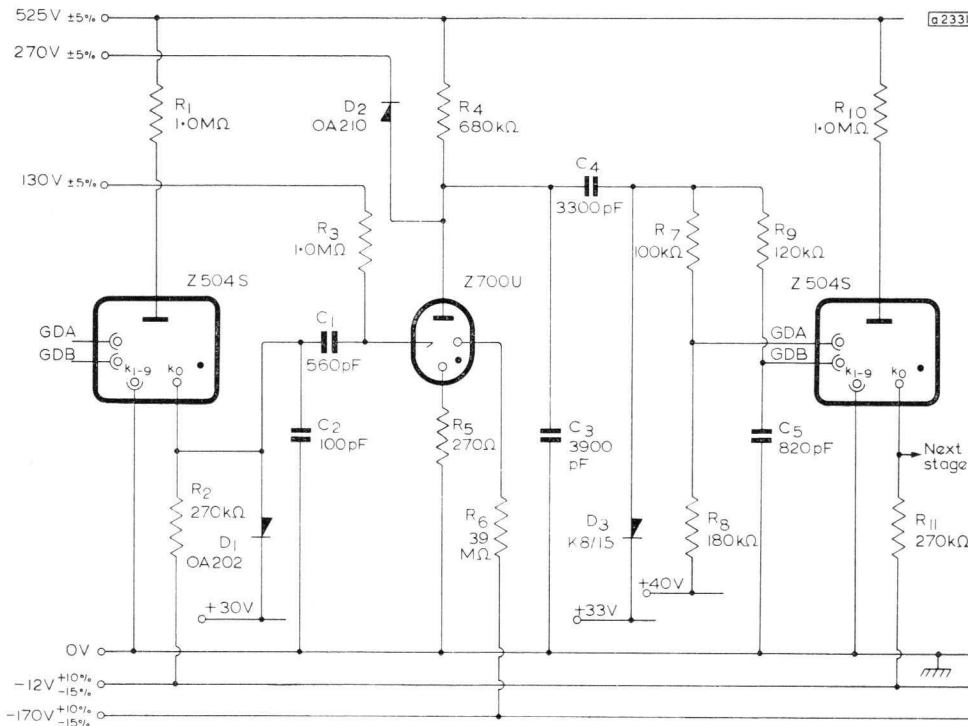


Fig. 6—Practical 400c/s coupling stage  
 $R_1, R_7, R_8, R_9, R_{10}$  are  $\frac{1}{4}\text{W}$ ,  $\pm 7\%$  total excursion  
 $R_2, R_3, R_4, R_5, R_6, R_{11}$ , are  $\frac{1}{4}\text{W}$ ,  $\pm 10\%$   
 $C_3$  is  $\pm 2\%$ . All other capacitors are  $\pm 10\%$

output voltage rises rapidly to the potential of the guide B cathodes, but is then clamped at this level by current-sharing between the main and guide cathodes. The output voltage then rises to its full value at the same rate as the trailing edge of the guide B pulse. To avoid a loss in output pulse due to capacitor C<sub>1</sub> charging through R<sub>3</sub>, the rise-time at the end of the guide B pulse to the first stage, and hence the rate of rise of output voltage, should be limited to less than 50μs.

**Output Circuit**

There are two main changes in the pulse-shaping network.

- (i) The d.c. restoring diode D<sub>3</sub> is added to ensure that C<sub>4</sub> discharges completely after each pulse, so that the effective guide bias remains at 40V at the increased operating speed. The diode is an S.T.C. K8/15, which has a forward voltage drop of about 7V at the relevant current. To compensate for this voltage drop, the cathode of the diode is taken to +33V. The addition of D<sub>3</sub> also overcomes the objection to larger guide resistors; therefore R<sub>7</sub> and R<sub>8</sub> have been substantially increased to minimise the drop in pulse amplitude caused by the charging of C<sub>4</sub>.
- (ii) The Z700U anode recovery time has been reduced by returning R<sub>4</sub> to the counter tube h.t. line of 525V, instead of to 270V. The voltage at the anode is restricted to its original value by the incorporation of the clamping diode D<sub>2</sub> (OA210).

The values of R<sub>7</sub>, R<sub>8</sub>, R<sub>9</sub>, and C<sub>5</sub> are determined in a similar way to those of the corresponding components in the low-speed circuit.

**Performance of 400c/s Circuit**

Fig. 7 shows the practical guide A and guide B voltage waveforms obtained in the 400c/s circuit at nominal supply conditions. Performance figures are given in Table 2.

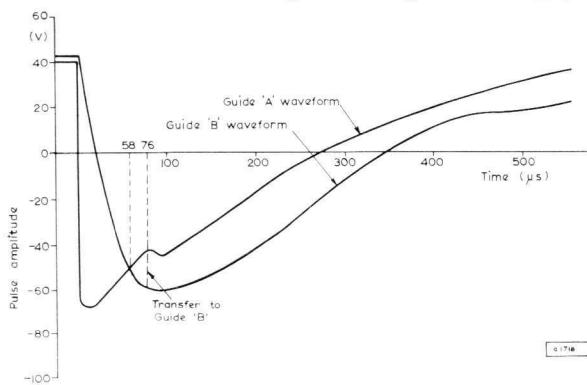


Fig. 7—Observed guide A and B waveforms (400c/s circuit)

These measurements have been made under the same operating conditions as for the 40c/s circuit, but at the maximum operating speed of 400c/s. Again, the results may vary from one Z700U to another by ±5%.

The crossover point will not have occurred within 58μs of the start of the guide A pulse. On the basis of life tests, this is known to be a reliable operating condition for this application. In most cases the guide A period of rest is greater than 60μs.

**TABLE 2**  
Performance of 0 to 400c/s Circuit

	SUPPLY VOLTAGES			
	Min.*	Nominal**	Max.†	
<b>Guide 'A'</b>				
Pulse amplitude	102	110	116	V
Typical period of rest	76	76	74	μs
Time for full recovery	640	640	640	μs
<b>Guide 'B'</b>				
Pulse amplitude	90	100	105	V
Typical period of rest	270	270	270	μs
Time for full recovery	800	750	950	μs
Time to crossover	58	58	58	μs

\*Positive supplies -5%, negative supplies -15%, frequency 400c/s.

\*\*Positive and negative supplies nominal, frequency 400c/s.

†Positive supplies +5%, negative supplies +10%, frequency 100c/s.

**AUXILIARY CIRCUITS**

Fig. 8 (p.190) shows three counter tubes, for counting units, tens, and hundreds at a maximum speed of 4kc/s. The first two tubes are coupled by the 0 to 400c/s circuit, and the second and third by the 0 to 40c/s circuit. The chain can be continued by the addition of further 0 to 40c/s coupling circuits.

This set-up requires, in addition, a 4kc/s drive circuit for the first counter tube, a power supply, and a system for resetting the counting tubes to zero.

**Drive Circuit**

The 4kc/s integrated-pulse drive circuits shown in the data sheets for the Z303C and Z502S can be used for driving the first Z504S in the Fig. 8 circuit.

**Power Requirements**

The following supply voltages are required in the 4kc/s counter circuit shown in Fig. 8, for up to six Z504S stages.

**TABLE 3**  
Power Requirements

Supply voltage (V)	Tolerance (%)	Current rating (mA)
525	±5	3
270	±5	0 to 1
130	±5	< 0.1
40	±5	0.5 to 1.5
33	±5	0 to 1
30	±5	0 to 1
-12	+10, -15	0 to 2
-170	+10, -15	< 0.1

To avoid spurious ignition under the top ceramic in the Z504S, it is recommended that the 525V supply be applied via a 1ms time-constant. With low-impedance supplies this may be accomplished with a 5kΩ series resistor and a 0.2μF shunt capacitor.

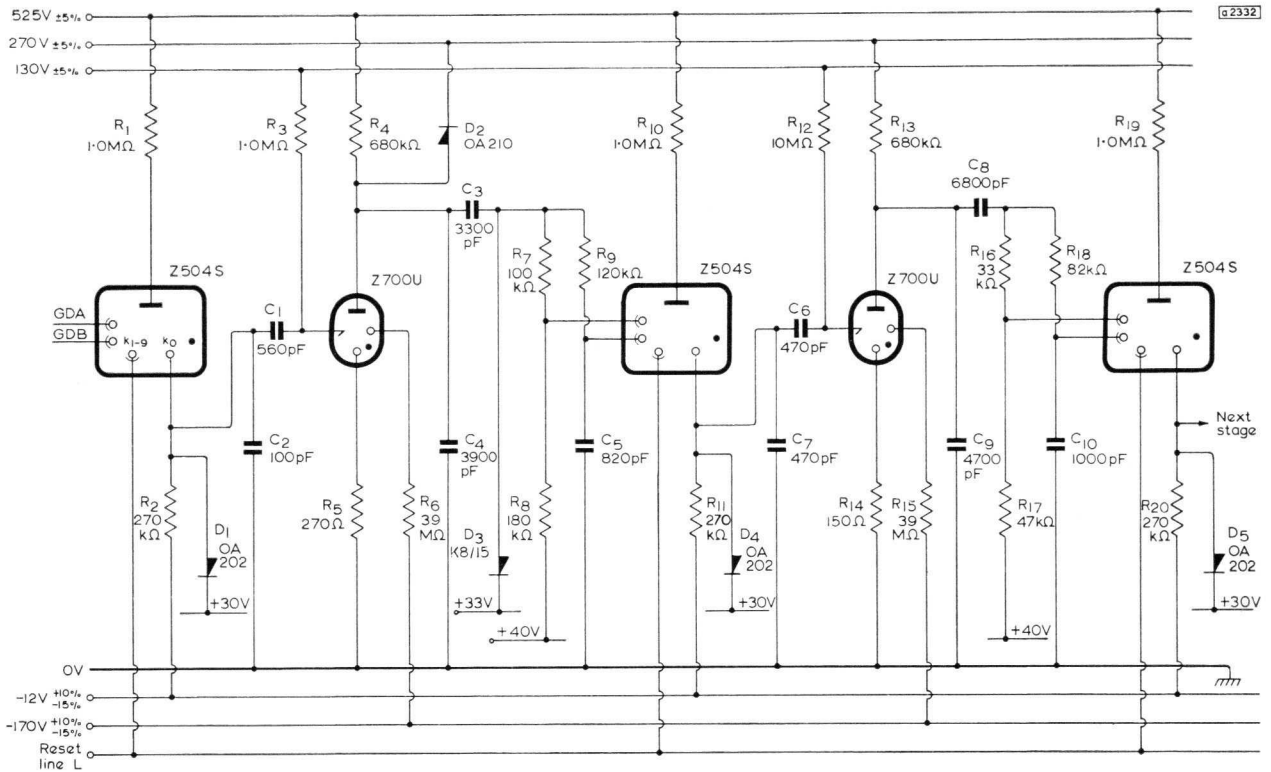


Fig. 8—Practical 4kc/s counter chain  
 $R_1, R_7, R_8, R_9, R_{10}, R_{16}, R_{17}, R_{18}, R_{19}$  are  $\frac{1}{4}W$ ,  $\pm 7\%$  total excursion  
 All other resistors are  $\frac{1}{4}W$ ,  $\pm 10\%$   
 $C_4$  is  $\pm 2\%$ . All other capacitors are  $\pm 10\%$

One method of obtaining these supplies is shown in Fig. 9. The potential divider network replaces a number of supply lines, so that only two positive and two negative supplies are required. A manual or electromechanical resetting circuit has been incorporated.

The potential divider network will modify the current requirements of the two positive supplies as follows:

- (i)  $+525V \pm 5\%$  at 17mA
- (ii)  $+130V \pm 5\%$ . About 2mA of current will flow into this supply during normal operation, and this will rise to approximately 12mA during resetting. The stabilised power unit must, with the arrangement shown in Fig. 9, be designed to accommodate this feedback of 12mA.

**POWER UNIT**

If the two positive and two negative supplies are not available, then the circuit shown in Fig 9 cannot be used, and a complete power supply is required. A suitable circuit is shown in Fig. 10.

This power supply provides  $+570V$ ,  $+270V$  (stabilised), and  $-180V$ , from the a.c. mains. The stabilised 270V supply is followed by a potential divider network from which are derived the intermediate positive voltages.

To avoid the use of a separate  $-12V$   $k_0$  bias supply, the d.c. levels have where necessary been increased by 12V.

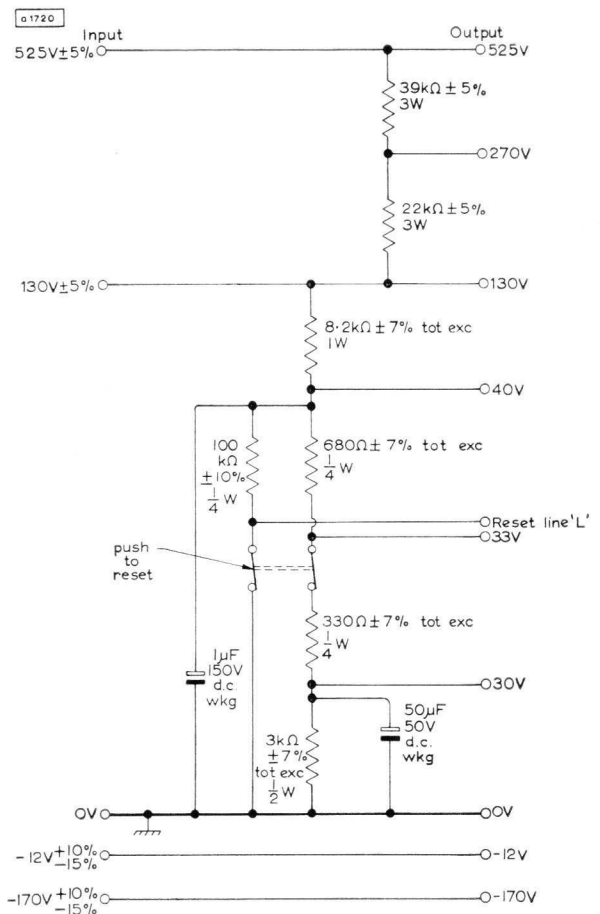


Fig. 9—Derivation of voltage rails from two positive and two negative supplies. A resetting circuit is included



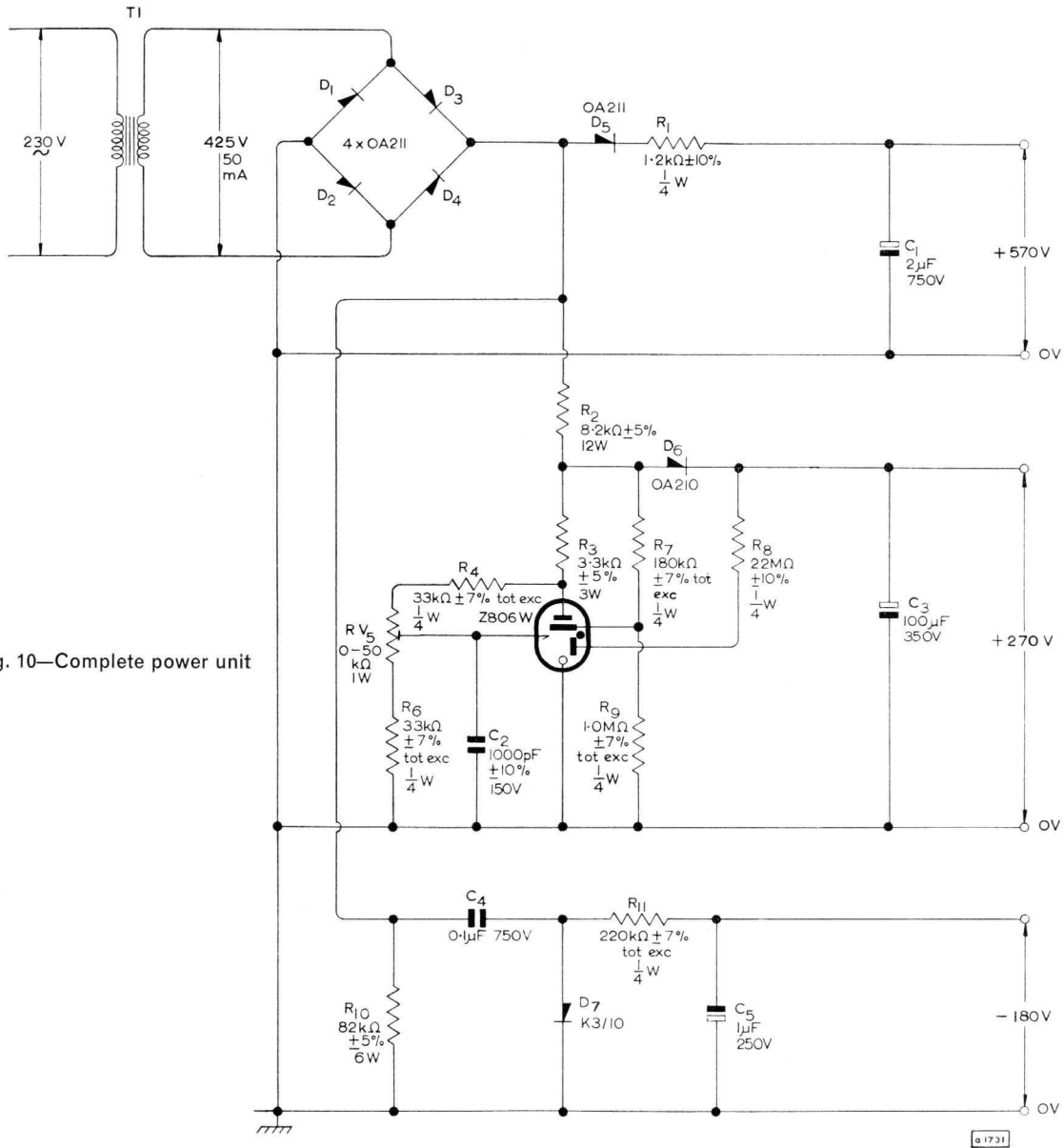


Fig. 10—Complete power unit

With this arrangement, the  $k_0$  resistors are returned to zero volts, and the  $k_{1-9}$  cathodes to +12V; the output cathode reference level becomes 42V, and the positive guide bias is increased to 52V.

**Stabilised 270V Supply**

The central part of the power unit consists of a Z806W stabiliser circuit which provides a 270V stabilised supply to the potential divider network in Fig. 11 (p.192).

The full-wave rectified voltage output from the bridge (Fig. 10) charges the reservoir capacitor  $C_3$  through  $R_2$  and  $D_6$ . When the potential of  $C_3$ , and hence the anode of the Z806W, rise to a predetermined value (in this case 270V), the trigger ignition voltage is exceeded and the tube fires. The voltage at the junction of  $R_2$  and  $R_3$  then falls, and  $D_6$  becomes reverse-biased; so that throughout the remainder of the half-cycle all the circuit current flows through the Z806W and no more charge is impressed on  $C_3$ .

In the off-load condition  $C_3$  cannot discharge, so that in the succeeding half-cycles of the mains, the Z806W fires as soon as the supply voltage reaches 270V and the diode  $D_6$  cannot conduct. Under these conditions all the circuit current continues to flow through the trigger tube, and the output voltage is stabilised at 270V. The value of the output voltage is determined by the very stable trigger ignition voltage of the Z806W and by the preset potential divider  $R_4$ ,  $RV_5$ , and  $R_6$ .

Consider the operation of the circuit when the output terminals are connected to a load. Initially, the Z806W anode voltage rises with the applied sinewave until the potential of capacitor  $C_3$  is reached, as shown in Fig. 12a. Diode  $D_6$  then conducts, and  $C_3$  is recharged through  $R_2$  until its potential reaches 270V. At this level the tube fires, and  $D_6$  is cut off once more. Capacitor  $C_3$  then discharges into the load, as shown by line 'C', until the next half-cycle, when the process is repeated.

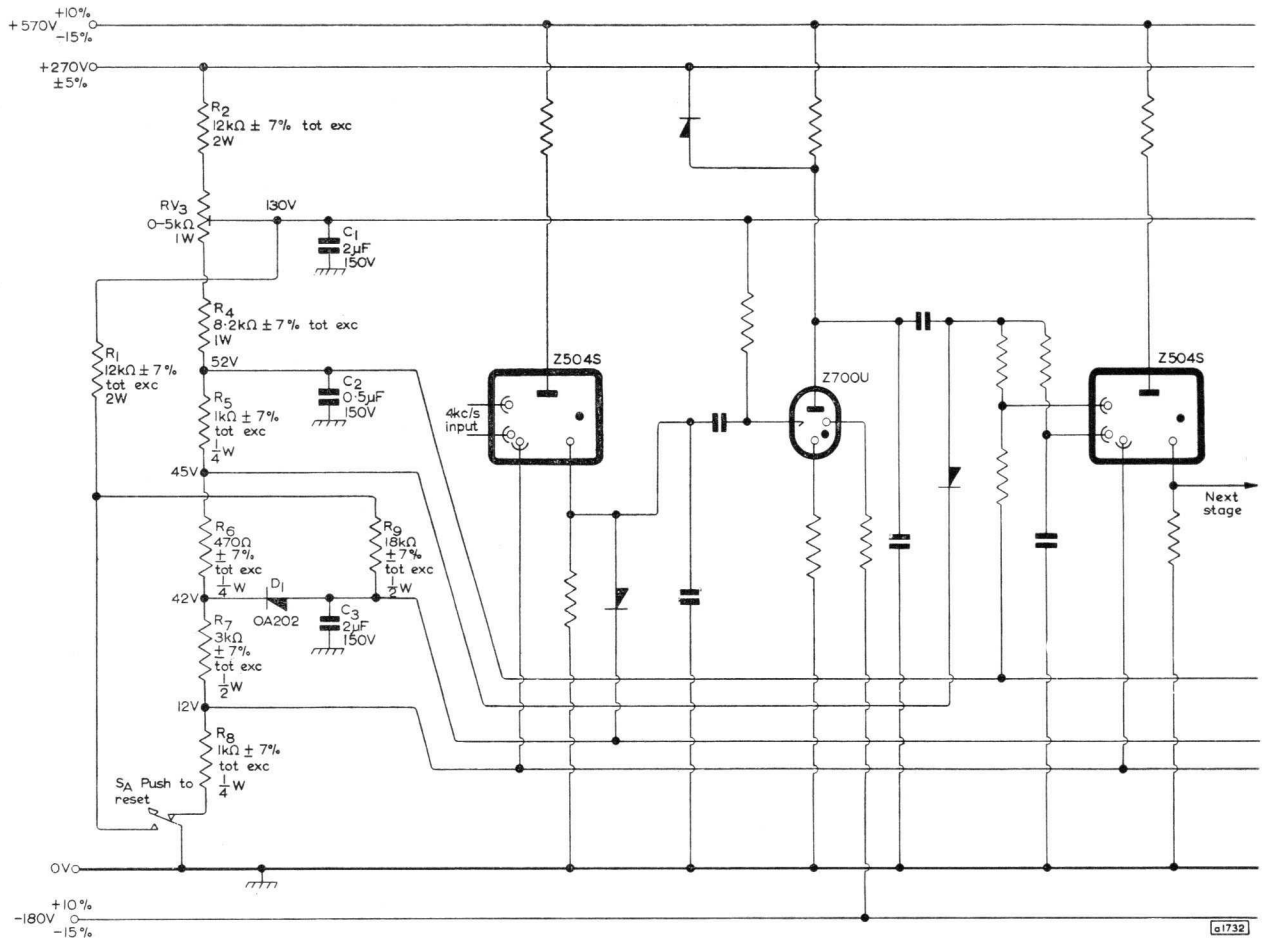


Fig. 11—Potential divider, modified voltage rails, and resetting circuit, connected to 4kc/s counter

It will be seen from a comparison of Fig. 12a with the off-load condition of Fig. 12b that the recharging of C<sub>3</sub> causes the Z806W to fire later in the half-cycle, so that the mean tube current decreases as the load current increases, thus giving the desired stabilising action.

In the present circuit, the stabiliser has been designed to operate over the current range 4.5 to 9.8mA. It is important not to operate the stabiliser off-load, otherwise the mean tube current limit will be exceeded.

**Unstabilised 570V Supply**

From the junction of D<sub>3</sub> and D<sub>4</sub> (Fig. 10) the full-wave rectified supply is taken to D<sub>5</sub>, R<sub>1</sub>, and C<sub>1</sub> to give a 570V unstabilised supply for the Z504S anodes and for the anode circuit of the Z700U in the first coupling stage. The increase of this h.t. line from 525V to 570V permits an unstabilised supply to be used, with mains voltage variations of +10% to -15%, maintaining voltage variations, and resistor tolerances taken into account.

Diode D<sub>5</sub> is included to permit the output of the bridge rectifier to fall to zero at the end of each half-cycle of the mains, so that the Z806W in the stabiliser circuit is extinguished.

Resistor R<sub>1</sub> slows the rate of rise of the Z504S anode

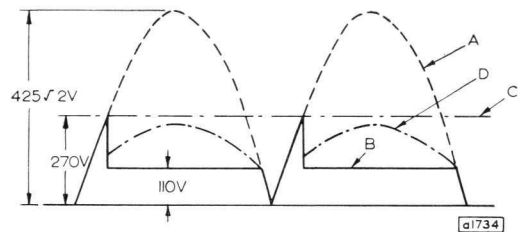
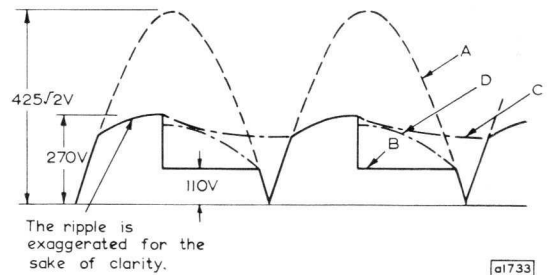


Fig. 12—Waveforms in stabilised power supply  
 Above: on load      Below: off load  
 A—bridge rectifier output voltage  
 B—anode voltage of Z806W  
 C—output voltage at C<sub>3</sub>  
 D—voltage at junction of R<sub>2</sub> and R<sub>3</sub>

voltage, and prevents spurious breakdown within the tube. The 550V published limit for the Z504S anode voltage is associated with switch-on. Although in the circuit shown here the nominal voltage is 570V, by using a long time-constant of 2.4ms (given by  $R_1 \cdot C_1$ ) the effective voltage up to the instant of establishing the discharge within the Z504S is less than 550V. Once the tube is conducting, there is no restriction on higher voltages, provided that the current limits of the tube are observed.

#### Unstabilised Primer Supply

The negative supply for the priming cathodes of the Z700U is obtained from a d.c.-restoring diode circuit driven from the output of the bridge rectifier. This circuit generates a nominal  $-180V$  supply at from 0 to  $100\mu A$ .

Although resistor  $R_{10}$  appears in the negative supply circuit, its purpose is to ensure that the potential at the output of the bridge falls below the maintaining value for the Z806W under all conditions of use. In the absence of  $R_{10}$ , the charge on capacitors  $C_4$  and  $C_5$  would hold the output voltage of the bridge rectifier above the maintaining value for the Z806W, so that it could not extinguish.

#### PERFORMANCE OF POWER UNIT

The three sections of the power unit have been designed to accommodate mains voltage variations of  $+10\%$  and  $-15\%$ . Table 4 shows the limit condition voltages, the peak-to-peak ripple voltages at nominal conditions, and the nominal current required from each supply by a six-stage counter.

If load variations are equal to the whole current range of 4.5 to 9.8mA for this stabiliser circuit, the output change is less than 1.5% about 270V, taking into account supply variations of  $-15\%$  and  $+10\%$ .

In conventional-type stabiliser circuits, the reference level depends on a resistive potential divider. It may drift slightly, and require adjustment, after long usage. In the present circuit, controls  $RV_5$  (Fig. 10) and  $RV_3$  (Fig. 11) are provided for resetting the 270V and 130V lines to their nominal values. The counter circuit design, however, permits  $\pm 5\%$  variations in these voltages before adjustment becomes necessary.

TABLE 4  
Performance of Power Unit

Nominal supply	Mains $-15\%$	Mains $+10\%$	Peak-to-peak ripple	Nominal current loading
+270V (stabilised)	+270V	+271V	0.8V	9.0mA
+570V (unstabilised)	+485V	+630V	12.0V	2.7mA
$-180V$ (unstabilised)	$-153V$	$-200V$	3.5V	0.05mA

#### OPERATION OF RESET

In Fig. 11, switch  $S_A$  is for resetting the counter tubes to zero. During counting, the potential divider chain is earthed by  $S_A$ . For reset, the 130V line is earthed via  $R_1$ , which has about the same value as the sum of  $R_4$  to  $R_8$ . Thus the 130V line is depressed slightly, whereas all guide and  $k_{1-9}$  cathodes are taken up to about  $+125V$ . The discharge will therefore transfer to  $k_0$  in all tubes.

To protect the diodes in the output cathode circuits against excessive peak inverse voltages, the  $k_0$  clamp diode voltage is disconnected from the potential divider, during reset, by  $D_1$ . The anode of  $D_1$  is returned to earth via  $R_9$ , and  $D_1$  is reverse-biased. The value of  $R_9$  is selected so that, with the  $k_0$  current of the stepping tubes flowing through it, the voltage at the anode of  $D_1$  is not greater than the normal value of 42V.

At the end of reset,  $S_A$  disconnects  $R_9$  from earth and returns  $R_8$  once more to earth. Capacitor  $C_1$  is included to stop the 130V line potential from increasing to 270V during the switch transit. Similarly,  $C_3$  restricts the rise of the  $k_0$  clamp voltage. Smoothing for the guide-bias line is provided by  $C_2$ .

#### REFERENCE

1. JEYNES, G. F. 'Decade Stepping Tubes and their Operation'. *Mullard Technical Communications*, Vol. 4, No. 37, Feb. 1959, pp. 194 to 208.

# Electrometer Valves

S. S. DAGPUNAR

Mullard Applications Research Laboratory

*This article gives general information on electrometer valves, including types of application and some recommendations relating to their use. Information obtained on the performance of Mullard ME1401, ME1402, ME1403 and ME1404 electrometer valves is given, showing the logarithmic characteristics, drift, and the electrical effects of vibration and shock. Some practical circuits employing these valves in both logarithmic and linear applications are shown.*

## INTRODUCTION

An electrometer valve is a high-vacuum valve designed to have a very low control grid leakage to facilitate the measurement of extremely small direct currents or voltages. The present range of electrometer valves consists of:

ME1401, ME1404	Triodes
ME1402	Space-charge grid tetrode
ME1403	Pentode

Currents in the region of  $10^{-9}$  or  $10^{-10}$ A can be measured by means of semi-electrometer valves, such as the E80F or ME1400, which are derived from conventional receiving valves.

Small d.c. currents down to  $10^{-15}$ A, or small d.c. voltages from a high impedance source, can be measured with the aid of specially designed valve electrometers which have directly heated filaments and are generally subminiature types, or vibrating reed (capacitor) electrometers. The advantages of valve electrometers are cheapness, simplicity, portability and suitability for logarithmic applications. Their disadvantages are their lower current sensitivity and lower stability, compared with vibrating reed electrometers.

The properties desired in an electrometer valve are low grid current ( $10^{-15}$  to  $10^{-13}$ A, depending on requirements); freedom from objectionable interference, including instability, drift and microphony; and, for logarithmic applications, a high number of decades of logarithmic performance (up to eight decades, depending upon individual requirements). To obtain a low grid current, a low leakage is essential. Because of the low leakage requirement, a minimum number of electrode supports are required, which increases the sensitivity to instability, drift, and microphony. Therefore a compromise must be made in the design of electrometer valves; and, in order to realise or approach ideal operating conditions, the valves should be used when certain precautions have been taken.

Fig. 1 illustrates grid current and its components versus grid voltage, and also the causes of these components (Ref. 1).

The present article outlines techniques for obtaining optimum performance from electrometer valves.

## APPLICATIONS

Electrometer valves are used as the input stage of a high impedance amplifier. They may be used in a linear or logarithmic manner as described below.

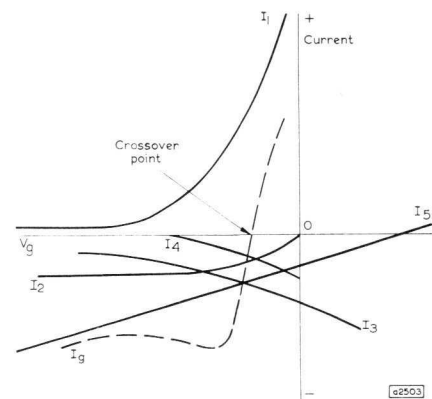


Fig. 1—Variation of grid current and its components with negative grid voltage

- $I_1$ —Electrons from the cathode
- $I_2$ —Positive ions from the cathode, thermionic and photo-emission from the grid, ionisation of gas by soft x-rays produced at the anode by arriving electrons.
- $I_3$ —Positive ions formed in gas by accelerated electrons or those released from the heated anode by bombarding electrons
- $I_4$ —Secondary electrons from the grid bombarded by positive ions
- $I_5$ —Leakage over glass, or insulation, both inside and outside the valve

## Logarithmic Application

Logarithmic operation for current measurement increases the range of current measurement without the necessity for manipulating a range switch. In logarithmic application the current to be measured is fed from a current source directly to the grid of the valve. The valve has no grid leak resistance and operates as a current amplifier. (Figs. 2 and 3.) The control grid is positive with respect to the crossover point (Fig. 1); therefore, the grid current consists mainly of electron current ( $I_1$  in Fig. 1). With the grid negative with respect to cathode, the grid-cathode system acts as a retarding field diode causing the grid current to vary exponentially with the negative grid voltage. This results in the grid voltage

being proportional to the logarithm of grid current.

From this basic relationship and from the known characteristics of thermionic valves further practical relationships can be derived.

For instance, in the case of triodes, assuming that the mutual conductance remains reasonably constant over the required range and at constant anode voltage, the grid voltage is proportional to the anode current. Consequently, the logarithm of the grid current is proportional to the anode current. Similarly, if the anode current is kept constant by varying the anode voltage, the anode voltage is proportional to the grid voltage and therefore the logarithm of the grid current is proportional to the anode voltage.

In the case of pentodes, assuming that the anode current is kept constant by varying the screen grid voltage, the control grid voltage is proportional to the screen grid voltage. Therefore the logarithm of the control grid current is proportional to the screen grid voltage.

However, there are limitations to logarithmic performance at both the low and high current ends of the scale. At low values of positive grid current, the  $I_g$  curve departs from the exponential curve  $I_1$  (Fig. 1), because of the influence of the other components of grid current. Thus the minimum positive grid current that can be used in logarithmic applications is approximately the same as the negative grid current used in normal (linear) operation. Experimental results show that at high values of positive grid current the departure from logarithmic relationship occurs either when the grid is positive with respect to

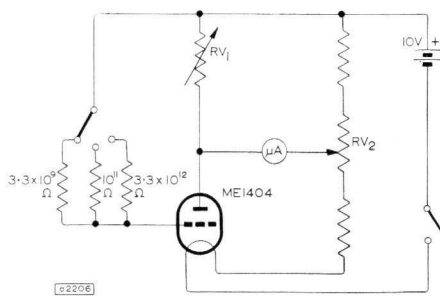


Fig. 2—ME1404 test circuit

cathode (hence the exponential law for  $I_1$  becomes a three halves power law) or when the grid current is comparable to the anode current. The limitation which has the most effect depends upon the valve type and the circuit used. For example, the ME1403 is restricted mainly by the second effect; but the ME1402, with its much higher anode current, is limited by the first effect.

#### Linear Application

Linear application is used for both current and voltage measurements. In this application, the required grid bias is approximately one or two volts negative with respect to the crossover point.

With the use of appropriate circuit techniques, linear application can be used, either for current or voltage measurements. For current measurements, either the voltage-drop or the capacitor charging method is used

(Ref. 2). In the first method, the current to be measured is passed through a high resistance of known value. The voltage drop across this resistor is measured by the electrometer valve, and the current is determined by Ohm's Law. In the second method, the input current is effectively added to the grid current. The corresponding rate of change of grid potential is derived from the accompanying anode current variation, and the input current is determined by multiplying the rate of change of grid potential by the total input capacitance. For voltage measurements, the input is fed from a voltage source. A grid leak resistor may be required but this depends on the source impedance.

#### PRACTICAL CIRCUITS

Some practical circuits using electrometer valves are given in Figs. 2 to 5. In Figs. 2 and 3 the valves are operating in logarithmic mode and in the remaining circuits in linear mode.

The circuit in Fig. 4 uses slide-back principles. With no input current, the reading on voltmeter V is brought to zero by adjusting  $RV_1$ . The reading on galvanometer G is set at zero by adjusting  $RV_2$ . The input current is applied and  $RV_1$  is adjusted to bring the galvanometer reading back to zero. The reading on the voltmeter is noted. The input current is then determined by applying Ohm's Law to the voltmeter reading and the grid leak resistance  $R_g$ .

Fig. 5 shows a balanced circuit designed to minimise the effect of variations in supply voltages (Ref. 3). Fig. 2

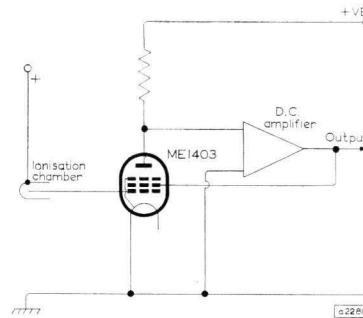


Fig. 3—ME1403 circuit

shows a basic valve test circuit. The calibration is made by successively injecting  $3 \times 10^{-12}$  and  $3 \times 10^{-9}$  A and adjusting  $RV_1$  for zero and  $RV_2$  for full scale deflection. The procedure is repeated several times to correct the effect of interaction of the potentiometers.

Fig. 3 shows an arrangement where the d.c. amplifies controls the screen grid voltage in a manner which tends to keep the anode voltage, and hence the anode current, constant. This method results in a logarithmic relationship between the screen grid voltage and the control grid current (Ref. 4).

#### PERFORMANCE OF MULLARD ELECTROMETER VALVES

The results quoted were obtained on small numbers of valves of each type, and are not, therefore, necessarily

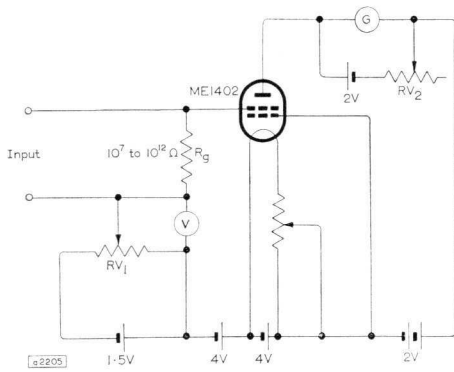


Fig. 4—Slide back method using ME1402

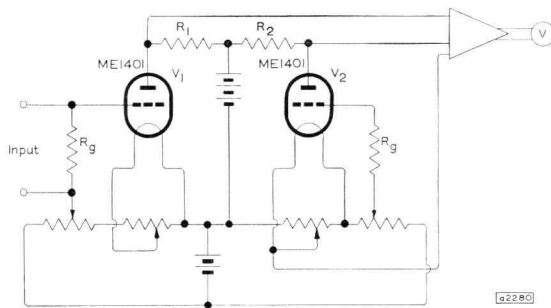


Fig. 5—Balanced triode circuit using ME1401

representative of every individual electrometer valve.

Because of the special circumstances in which the information has been obtained, equal effort has not been placed on each valve type and in particular it will be noticed there are fewer details on the ME1404, which has the widest tolerance.

The ME1404 is a similar type of valve to the ME1401. The spreads in results obtained on the ME1404 are likely to be similar to those shown in the ME1401. Generally, the ME1401 gives a better electrical performance than the ME1404.

#### Logarithmic Performance

As discussed under *Applications*, there are certain practical logarithmic relationships between input and output characteristics. Figs. 6a, 6b, 6c and 6d (page 197) illustrate the logarithmic performance of ME1401, ME1402, ME1403 and ME1404 valves. It can be seen that the approximate number of decades of logarithmic relationship is six for the ME1401, eight for the ME1402, seven for the ME1403, and three for the ME1404.

#### Vibration and Shock

Figs. 7 and 8 (page 198) show the electrical effect of vibration and shock on ME1401, ME1402, ME1403 and ME1404 valves. Normally, as shown in Figs. 8a, 8b, 8c and 8d (page 198) after the application of a shock, the d.c. anode current is shifted from its initial value and a damped a.c. component is superimposed whose frequency is equal to the natural frequency of the valve filament. These results indicate three important facts:

- (i) Electrometer valves are extremely sensitive to vibration or shocks.
- (ii) Mechanical shocks or vibration may result in a permanent change in the valve geometry, with corresponding changes in valve characteristics.
- (iii) All other factors being kept constant, the space-charge grid tetrodes (ME1402) are less sensitive to vibration and shock than conventional triodes.

#### Drift

Figs. 9a, 9b, 9c and 9d (page 199) give the short and long term drift characteristics obtained on typical ME1401, ME1402, ME1403 and ME1404 valves. The short term drift measurements were made by first applying the rated operating voltages and then taking current readings at five minute intervals for approximately thirty minutes.

The short term drift measurements were followed immediately by long term drift measurements. The intervals between successive readings were thirty minutes for the first sixteen readings and sixteen hours for the last two readings. At the start of the long term measurements, the operating voltages were adjusted to published data conditions. Then, before each reading, these voltages were adjusted (if different from the initial settings) to the values used at the start of the long term measurements.

#### GENERAL PRECAUTIONS TO MINIMISE GRID CURRENT IN A THERMIONIC VALVE

Fig. 1 shows the various components of grid current, which can be minimised in the following ways.

- (i) Electrons from the cathode, by using sufficiently high negative grid bias;
- (ii) positive ions from the cathode, by using a low value of heater voltage or by using space-charge grid valves;
- (iii) thermionic emission from the grid, by using a low value of heater voltage;
- (iv) photo-electric emission from the grid, by using a low value of heater voltage and also by screening the valve against external light;
- (v) leakage across the surface of the envelope, by keeping the valve clean and dry;
- (vi) all the remaining components, including  $I_3$ , by operating the valve at sufficiently low inter-electrode voltages.

The published operating conditions for each valve type take these facts into consideration.

With the heater and supply voltages applied to the valve, the grid current depends greatly on the photo-electric emission and leakage components. For example, experiments carried out on one ME1402 valve operating at rated voltages show that the negative grid current rises from its initial value of  $1.3 \times 10^{-15} \text{A}$  in complete darkness to about  $10^{-13} \text{A}$  in room lighting. When the same valve is replaced in its light-tight box after being contaminated with dust and humid air, the grid current rises from  $1.3 \times 10^{-15} \text{A}$  to  $3 \times 10^{-13} \text{A}$ . Nielson states (Ref. 5) that a  $\frac{1}{4}$ -inch diameter hole in a box containing the valve gives a photo-electric current of  $10^{-12} \text{A}$  in some instances, because of room lighting.

PERFORMANCE\_GRAPHS

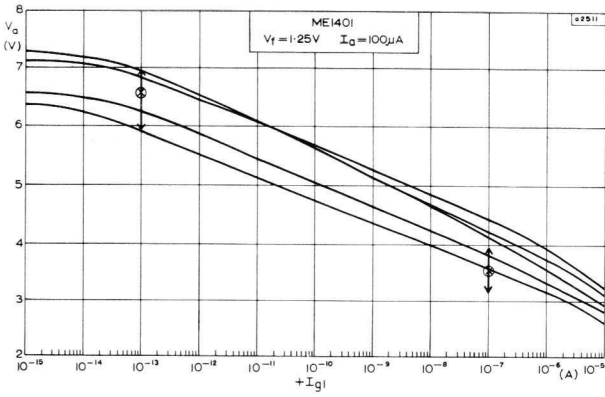


Fig. 6a

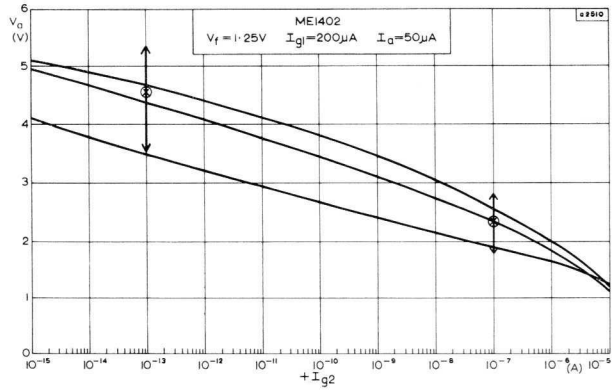


Fig. 6b(i)

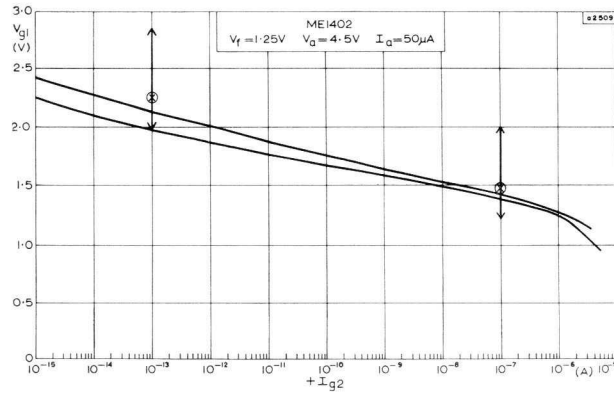


Fig. 6b(ii)

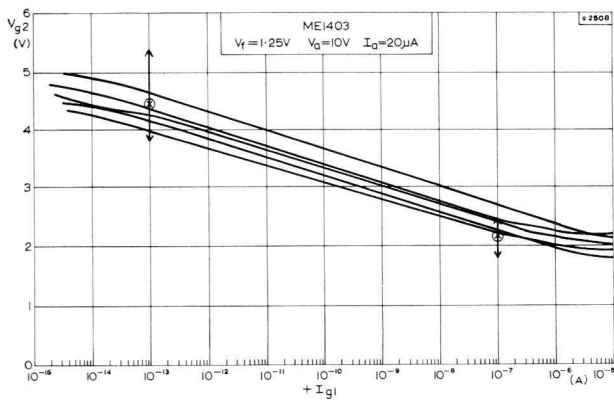


Fig. 6c

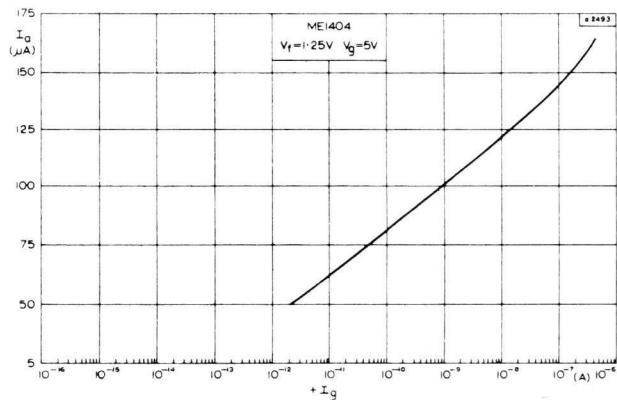


Fig. 6d

Results obtained on typical valves when logarithmic application is used. Vertical arrows indicate the spread obtained on 25 valves. Median values indicated by ringed crosses

ELECTROMETER VALVES

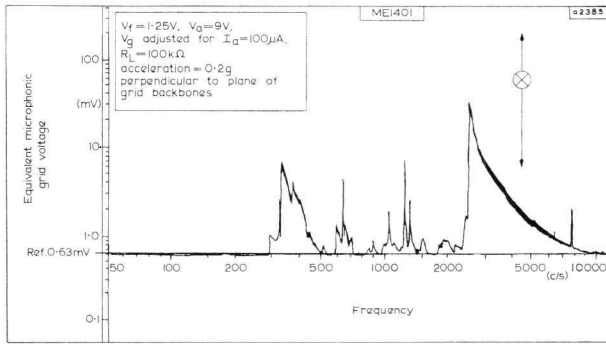


Fig. 7a

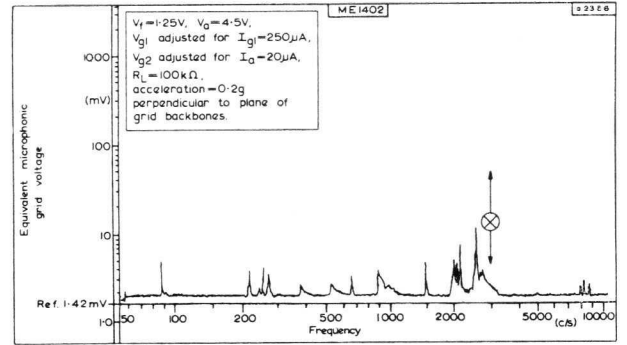


Fig. 7b

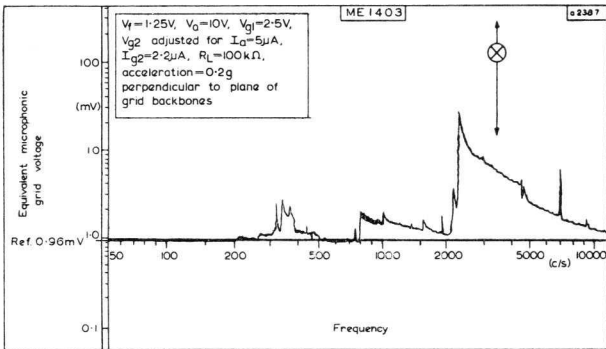


Fig. 7c

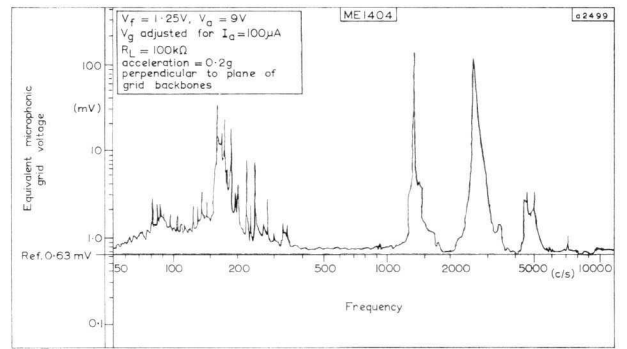


Fig. 7d

Typical microphony versus excitation frequency characteristics. Vertical arrows indicate the spread obtained on 25 valves. Median values indicated by ringed crosses

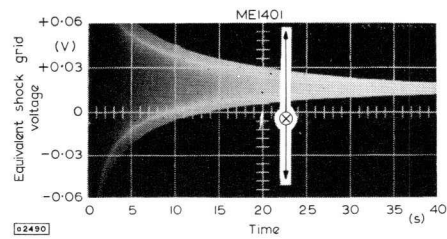


Fig. 8a

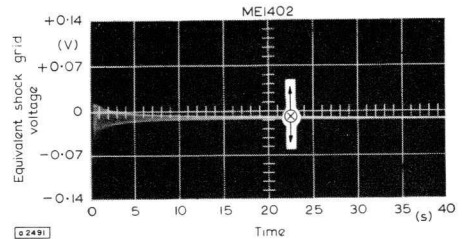


Fig. 8b

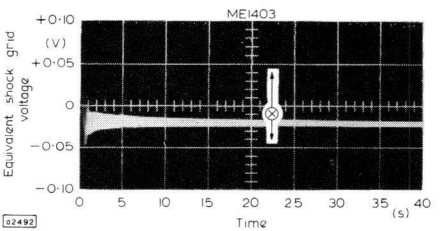


Fig. 8c

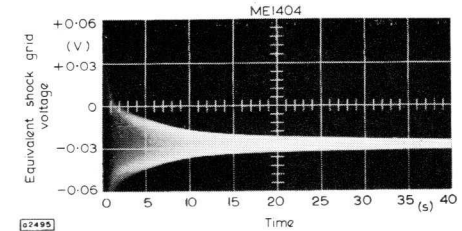


Fig. 8d

Typical results of shock excitation tests. Vertical arrows indicate the spread obtained on 25 valves. Median values indicated by ringed crosses



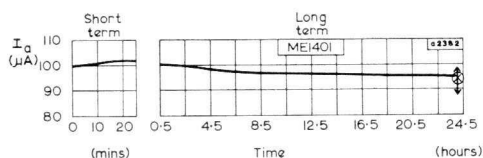


Fig. 9a

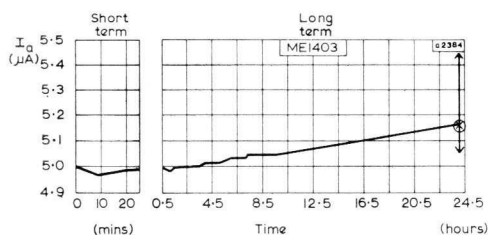


Fig. 9c

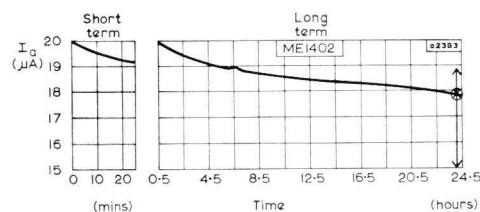


Fig. 9b

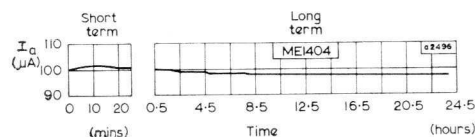


Fig. 9d

Drift characteristics of typical valves. Vertical arrows indicate the spread obtained on 25 valves. Median values indicated by ringed crosses

The main causes of common troubles (interference, instability, drift, microphony, etc.) are:

- (i) pick-up from stray fields or radiant energy;
- (ii) supply voltage variations;
- (iii) changes in values of components;
- (iv) circuit contact potentials;
- (v) long time-constants in the circuit;
- (vi) failure to allow thermal equilibrium to be attained;
- (vii) poisoning of emission mechanism;
- (viii) temporary or permanent changes in inter-electrode spacings in the valve structure;
- (ix) surface leakage due to contamination or mishandling.

Some practical precautions to minimise the grid current and the above mentioned undesirable phenomena can be summarised in relation to the valve, its supply voltages, and the circuit components.

#### Valve

The valve should be kept clean in a protective covering until it is ready for use. Particular precautions that should be taken are that the valve should be handled by the top half of the envelope, and mounting supports should only come in contact with the top half of the valve. Care should be taken to prevent resin coming into contact with the envelope during soldering. If contamination has occurred, however, the valve should be washed in alcohol.

The valve should be used within the operating voltages given in published data. It should be enclosed in a metal box which acts as a screen against electric and magnetic fields and against all likely forms of radiant energy (including light, gamma rays, x-rays and high energy particles such as deuterons, protons and electrons). Where the full performance of the electrometer valve is required the box should be air-tight and dry.

It is recommended that the electrometer valve should be operated for thirty minutes before measurements are made in order to reach thermal equilibrium. The valve,

with its associated equipment and leads, should be protected from any mechanical or acoustical excitation.

#### Supply Voltages

Many applications using electrometer valves are for d.c. amplifiers. Because of the output stability requirement it is necessary to use well stabilised supply voltages or large capacity batteries. It may be necessary for a suitably balanced circuit to be used to reduce the effect of supply voltage variations.

To prevent contamination of the emission mechanism, the filament voltage should be applied before the anode and screen grid voltages.

#### Components

Preferably, all essential insulation should be screened to avoid interference from varying potentials. All surfaces where high insulation is not required should be preferably coated with a conductive material to prevent the accumulation of charge. Because of the very high impedance associated with the grid circuit, it is only possible to use high quality components in the input circuit.

#### REFERENCES

1. YARWOOD, J., LE CROISSETTE, D. H., 'D.C. Amplifiers'. *Electronic Engineering*, Vol. XXVI, No. 311, Part I, Jan. 1954, pp. 14 to 19, No. 312, Part II, Feb. 1954, pp. 64 to 70.
2. JERVIS, M. W., 'The Measurement of Very Small Direct Currents'. *Electronic Engineering*, Vol. XXVI, No. 313, Mar. 1954, pp. 100 to 105.
3. BÖHM, H., 'Elektrometrische Betriebsmessgeräte', *Archiv Technische Messen*, Oct. 1959, No. 285, pp. 217 to 220.
4. COX, R. J., 'Automatic Start-up of Nuclear Reactors'. *I.R.E. Transactions on Nuclear Science* (Professional Group on Nuclear Science), Vol. NS-3, No. 1, Feb. 1956, pp. 15 to 20.
5. NIELSON, C. E., 'Measurement of Small Currents: Characteristics of Types 38, 954, and 959 as Reduced Grid Current Tubes'. *Review of Scientific Instruments*, Vol. 18, No. 1, Jan. 1947, pp. 18 to 31.





**MULLARD LIMITED**

Mullard House  
Torrington Place  
London, W.C.1

**CONTENTS**

Elimination of Switch-off Spots in TV Receivers	170-171
Junction Temperature of Diodes in Harmonic Generators	172-174
Design of High-impedance Common-collector Input Stages	175-178
Dual Trace Oscilloscope Tubes	179-183
Trigger Tube Coupling Circuits for Counting Tubes	184-193
Electrometer Valves	194-199

